Low-Speed Aerodynamic Performance of an Eppler 212 Wing With Variable Winglet Configurations

Gabriel R. Shupe*
Ira A. Fulton School of Engineering, Tempe, AZ, 85281

This study investigates the aerodynamic effects of several winglet configurations applied to an Eppler 212 finite wing in low speed wind tunnel conditions. The objective was to evaluate how winglet angle, length, and placement influence lift, drag, and overall aerodynamic efficiency. Experimental procedure was performed in which gravitational biases were removed, the wing was tested across a range of angles of attack, and data were collected at two Reynolds numbers representative of low-speed flight. Lift and drag coefficients were computed from force-balance measurements, and uncertainties were accounted for using standard propagation methods. The results show that all winglet configurations increased lift relative to the control wing and consistently reduced induced drag, improving aerodynamic efficiency. Differences among winglet families were present: moderate angles, longer winglet, and configurations mounted furthest back produced the largest increase in efficiencies. Increasing Reynolds number strengthened these effects by delaying flow separation and reducing drag. These findings align with theory and reflect the same methodology used in practical aircraft design to enhance performance and efficiency.

I. Nomenclature

C_L	=	lift coefficient
C_D	=	drag coefficient
dC_L	=	uncertainty in lift coefficient
dC_D	=	uncertainty in drag coefficient
L	=	lift force (N)
D	=	drag force (N)
F_N	=	normal force measured by balance (N)
F_A	=	axial force measured by balance (N)
μ	=	dynamic viscosity ($\mathrm{kg{\cdot}m^{-1} \cdot s^{-1}}$)
μ_{ref}	=	reference viscosity at T_{ref} ($\mathrm{kg{\cdot}m^{-1} \cdot s^{-1}}$)
$\delta\mu$	=	uncertainty in viscosity ($\mathrm{kg{\cdot}m^{-1} \cdot s^{-1}}$)
P	=	static pressure (kPa)
q_∞	=	freestream dynamic pressure (Pa)
δq_∞	=	uncertainty in freestream dynamic pressure (Pa)
Re	=	Reynolds number
S_{Suth}	=	Sutherland's constant (K)
S	=	wing planform area ($\mathrm{m^2}$)
T	=	freestream temperature (°C or K)
T_{ref}	=	reference temperature for Sutherland's Law (K)
α	=	geometric angle of attack (deg)
α_{true}	=	corrected angle of attack (deg)
$\delta\alpha$	=	uncertainty in angle of attack (deg)
c	=	airfoil chord length (m)
b	=	airfoil span (m)
ρ	=	air density ($\mathrm{kg{\cdot}m^{-3}}$)
$\delta\rho$	=	uncertainty in air density ($\mathrm{kg{\cdot}m^{-3}}$)

*Student, Arizona State University, Ira A. Fulton School of Engineering, 699 S. Mill Ave 119, Tempe, AZ 85281

II. Introduction

Aerodynamic drag arises in several ways, and this experiment isolates the components acting on a finite wing through various winglet designs. The total drag force acting on the model consists of pressure drag, viscous drag, and induced drag generated by the wingtip vortex. In this experiment, drag is measured indirectly through the wind-tunnel force balance, which records the normal force, F_N, and the axial force, F_A. These are fit into lift and drag using the equations for lift and drag projection,

$$L = F_N \cos\alpha - F_A \sin\alpha, \qquad D = F_N \sin\alpha + F_A \cos\alpha \tag{1}$$

From these forces, the aerodynamic coefficient are defined as

$$C_L = \frac{L}{q_\infty S}, \quad \text{and} \quad C_D = \frac{D}{q_\infty S} \tag{2}$$

where

$$S = c \cdot b \tag{3}$$

is the planform area, and

$$q_\infty = \frac{1}{2}\rho V^2 \tag{4}$$

is the free stream dynamic pressure.

A finite wing generates a tailing vortex due to pressure difference between the upper and lower surfaces. This induces downwash behind the wing and upwash ahead of it, tilting the local flow downward. The downwash reduces the effective angle of attack and increases induced drag, while the upwash influences the incoming flow. This experiment measures how winglets alter this vortex system, thereby modifying lift and drag.

Although the Eppler 212 is a low-speed airfoil, the concepts that govern supercritical airfoil behavior still carry over. Supercritical airfoils feature a flattened upper surface and rear-loaded curvature to weaken the shock formation at near supersonic speeds [33]. In contract, standard cambered airfoils such as the Eppler 212 concentrate curvature on the front, producing a pressure difference and thereby high lift at low Reynolds numbers. Additionally, a higher camber increases lift at the cost of pressure drag and an increased chance for flow separation. These principles help contextualize how winglet geometry interacts with the airfoil efficiencies.

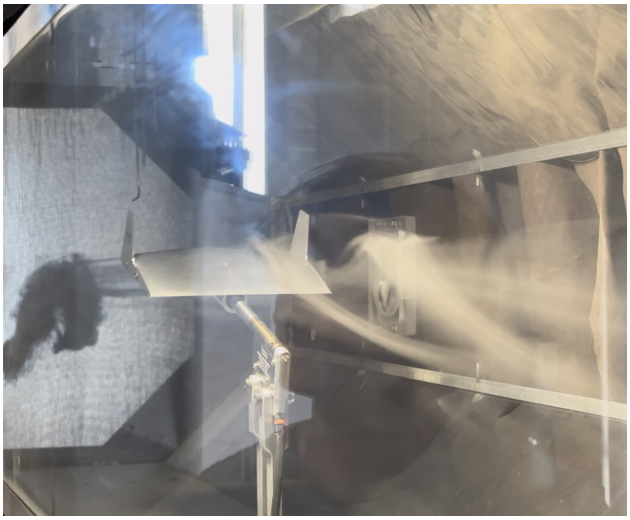

Fig. 1 Vortex Demonstration for Eppler 212

To define, a winglet is a small, vertically oriented surface added to the wingtip to redirect the spanwise flow that feeds directly into the wingtip vortex. Without a winglet, high pressure air from the lower surface curls around the tip, bleeding high pressure air into the low pressure region above, forming a strong vortex as the wing moves through the air. A winglet weakens this vortex by reducing the pressure leakage, which effectively increases the wings aspect ratio without increasing span.

By reducing the strength of the wingtip vortex, winglets directly decrease induced drag, especially at the moderate to high values for C_L. This increases aerodynamic efficiency and raises the lift curve without impacting the geometric angle of attack. Winglet may also introduce additional profile due to their inherent increase in wing area, so the net benefit depends on geometry, placement, and angle to influence effectiveness.

The three families of winglet variations examined in this experiment are as follows: angle, length, and location. Each family had three variations, angles of 20°, 40°, and 60, lengths of small, medium, and long, and placement locations from front, middle, to back of the airfoil. Each configuration influences the vortex path and the distribution of the pressure loading. Longer winglets reduce induced drag more effectively, moderate angles minimize profile drag, and winglets on the back end of the airfoil show strong benefits from to keep the leading-edge pressure in tact.

The aerodynamic condition of each test is characterized by the Reynolds number. The Reynolds number describes viscous forces in a flow. It determines the stability of the air flow around an airfoil. A low Reynolds number constitutes as laminar flow, which is essentially very organized streamlines of air prone to separation. Turbulent flow, on the other hand, is defined by a high Reynolds number and can be beneficial for preventing penalties derived from flow separation. In this experiment, Reynolds number is needed to compare data across multiple winglet configurations and ensure each case was tested under known, constant aerodynamic conditions. Reynolds number is computed using

$$Re = \frac{\rho V c}{\mu}, \tag{5}$$

which requires accurate values of both air density ρ and dynamic viscosity μ.

To compute viscosity, Sutherland's law is used. Sutherland's law proves a standard model for air viscosity as a function of air temperature. Since ambient temperature is measured in this experiment, it is the basis for being able to relate several of our known conditions. It is known by the equation

$$\mu = \mu_{\text{ref}} \left(\frac{T}{T_{\text{ref}}} \right)^{3/2} \frac{T_{\text{ref}} + S_{\text{Suth}}}{T + S_{\text{Suth}}}. \tag{6}$$

which relates 3 different known constants to a given input of T. In the context of this experiment, Sutherland's law is just another equation that allows us to relate Reynolds number to a number of aerodynamic conditions and compare the effects of various winglet configurations. Necessary for Reynolds number, density is evaluated using the ideal gas equation,

$$\rho = \frac{P}{RT}. \tag{7}$$

Air density has an impact on every aerodynamic measure, but in the context of this experiment acts as a necessary piece for several equations used to calculate measures of comparison.

Uncertainty in C_L and C_D is determined through the standard propagation of error equation,

$$\delta f = \sqrt{\left(\frac{\partial f}{\partial x} \delta x \right)^2 + \left(\frac{\partial f}{\partial y} \delta y \right)^2} \tag{8}$$

For the purposes of this experiment, uncertainty for the lift and drag coefficients becomes

$$\delta C_L = \sqrt{\left(\frac{\partial C_L}{\partial F_N} \, \delta F_N \right)^2 + \left(\frac{\partial C_L}{\partial F_A} \, \delta F_A \right)^2 + \left(\frac{\partial C_L}{\partial \alpha} \, \delta \alpha \right)^2 + \left(\frac{\partial C_L}{\partial q_\infty} \, \delta q_\infty \right)^2} \tag{9}$$

The same expression is applicable for δC_D, though all partials must be swapped to match. This ensures that each plotted point reflect the experimental precision that is inherently limited by the various systems of measurement.

These relationships form the conversion between raw measurements and collected data into aerodynamic coefficients that will be used for analysis. This experiment connects several key concepts, including how induced drag forms wingtip vorticies, how geometric modifications such as winglets can alter downwash and efficiency, and how changes in Reynolds number shift aerodynamic conditions and overall performance of the airfoil. By testing multiple winglet families under controlled conditions, the experiment intends to isolate aerodynamic consequences for each configuration and determine whether any winglet caused a meaningful improvement over the control. Ultimately, the objective is to understand not only whether winglets improve efficiency, but which ones, why, and under what flow conditions those improvements become greatest.

III. Procedure

The experiment was performed in the ASU USE174 high-speed wind tunnel. It is designed to deliver a uniform, freestream flow through an octagonal inlet and square test section. The inlet contains a honeycomb shaped filter to straighten out airflow followed by multiple mesh screens to reduce turbulence. Upstream measurements of ambient conditions were obtained using a thermocouple and pitot-tube mounted inside the tunnel. These were used to measure static pressure and determine freestream density and dynamic pressure. The Eppler 212 wing model was mounted on a pitch-angle control mechanism connected to a force balance capable of resolving normal and axial forces. The balance was connected to a DAQ system ran through LabVIEW, which recorded forces, atmospheric conditions, and pitch angle for each test point. The following diagram illustrates all major components and their positions relative to the wind tunnel.

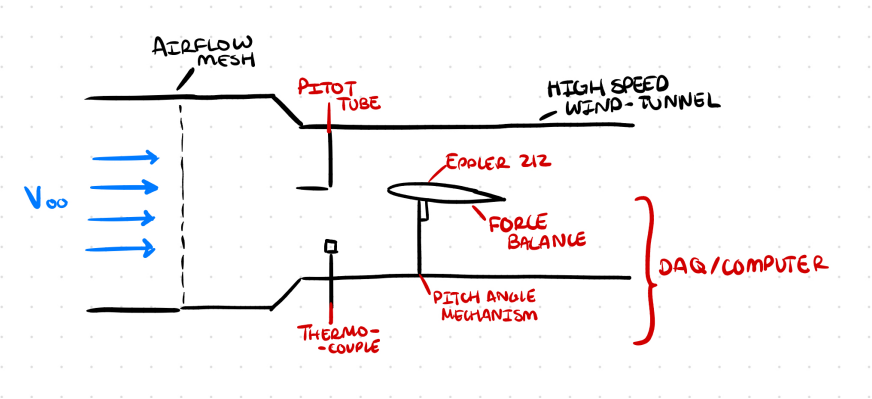

Fig. 2 Wind-Tunnel Diagram and Set Up

The force balance system used in this experiment is a strain-gauge based measurement system designed to resolve normal force F_N and axial force F_A acting on the wing. The model is mounted on a pitch-angle control mechanism attached to the balance, and aerodynamic loads create small deflections in the internals set for measurements. These deflections are measured by the strain gauges, which the DAQ converts into usable, calibrated force readings.

Because lift and drag do not align directly with the balance axes, the measured forces are rotated according to the pitch angle and offset. The offset is known to be -1.7°. The calculations for such are done through the standard equations for lift and drag (eqs. 1). A separate gravitational calibration run was performed with the tunnel turned off in order to measure the apparent forces caused by the models center of weight which varies at each pitch angle. These values were later subtracted from aerodynamic data to remove gravitational bias.

A consistent sequence was followed for each winglet configuration to ensure repeatability across all groups performing data collection.

1) Record ambient conditions: Temperature and static pressure were measured from the embedded thermocouple and pitot-tube to determine air density and viscosity.
2) Install the wing model: The Eppler 212 was mounted on the sting, and the pitch angle was adjusted so that the zero-lift orientation matches the reference for force balance.
3) Perform gravitational calibration: Tith the wind-tunnel off, the model was swept from -15° to 20° in 1° increments to record the gravitational offset forces for F_N and F_A. Test angles need to be adjusted by the known offset.
4) Set the tunnel to desired Reynolds number: The tunnel speed was adjusted to match the target Reynolds numbers, 150k and 300k, using velocity calculated from the pitot pressure.
5) Acquire aerodynamic data: Tt each pitch angle, F_N, F_A, temperature, pressure, and pitch-angle were recorded through LabVIEW.
6) Repeat for multiple winglet configurations: All steps were repeated for each configuration in the angle, length, and location families for both Reynolds numbers. A baseline control, Eppler 212 with no-winglet attached, was recorded as well.

The angle family includes 3 configurations, one at 20 degrees, 40 degrees, and 60 degrees. The length family configurations include small, medium, and long, and the location configurations include front, middle, and back.

Air density was computed for each wind-tunnel condition using the ideal gas relation (eqs. 7). Temperature readings were converted from Celsius to Kelvin. Uncertainty in density was obtained by standard propagation of error (eqs. 8),

which becomes

$$\delta\rho = \sqrt{\left(\frac{\partial\rho}{\partial P}\,\delta P\right)^2 + \left(\frac{\partial\rho}{\partial T}\,\delta T\right)^2},$$

with partials differentials of

$$\frac{\partial\rho}{\partial P} = \frac{1}{RT}, \qquad \frac{\partial\rho}{\partial T} = -\frac{P}{RT^2},$$

and measurement uncertainties

$$\delta P = 0.1 \text{ kPa}, \qquad \delta T = 1.0^\circ\text{C}.$$

This produced a single ρ and $\delta\rho$ values for each configuration. Standard, ambient conditions for each configuration are known [1].

Balance readings include gravitational bias from weight components acting along the measured axis. As stated, a separate gravity run was performed with the wind-tunnel off providing references values

$$F_{N,\text{grav}}, \quad F_{A,\text{grav}}, \quad \text{and} \quad \alpha_{\text{grav}}.$$

Each measured force and angle was corrected by subtracting the gravity run,

$$F_N = F_{N,\text{test}} - F_{N,\text{grav}}, \qquad \text{and} \qquad F_A = F_{A,\text{test}} - F_{A,\text{grav}}.$$

This isolates aerodynamic forces from gravitational bias.

Dynamic viscosity was computed using Sutherland's Law (eqs. 6) with known constants

$$\mu_{\text{ref}}, \quad T_{\text{ref}}, \quad S.$$

The Reynolds number for each test condition was then computed using the standard equation for Reynolds number (eqs. 5). The freestream velocity V was inferred from the known Reynolds number and chord length.

Corrected forces were transformed into aerodynamic lift and drag using the standard equations rotated for the true angle of attack,

$$\alpha_{\text{true}} = \alpha_{\text{test}} - 1.7^\circ.$$

Coefficients were computed using the standard equations for aerodynamic coefficients (eqs. 2) as well as calculated freestream dynamic pressure q_∞ (eqs. 4) and known wing area S (eqs 3).

Uncertainties for lift and drag coefficients were propagated through a known equation for each error (eqs. 9). The values for all partial derivatives were calculated, and the uncertainties are known to be

$$\delta F_N = \delta F_A = 0.005 \text{ N}, \qquad \delta\alpha = 0.25^\circ, \qquad \delta q_\infty = 0.5 \text{ Pa}.$$

All data processing is done through MATLAB functions utilizing loops. All code is referenced in Appendix C. A sample calculation for the processing described above is referenced in Appendix B. The data is plotted to form 6 C_L vs. α figures, one for each winglet family at either 150k or 300k Re, and each showing behavior for all 3 winglet configurations relative to the control. Additionally, the data is plotted to form 6 C_L vs. C_D figures known as drag polars, one for each winglet family at either 150k or 300k Re, and each showing behavior for all 3 winglets configurations. Vertical error bars in the plots for C_L vs. α represent δC_L. On the plots for C_L vs. C_D, vertical and horizontal error bars are included and reflect both calculated uncertainties.

IV. Results

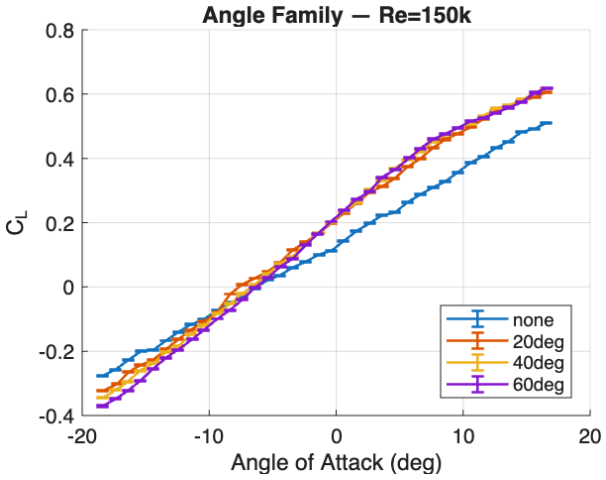

Fig. 3 C_L **vs.** α**, Angle, 150k Re**

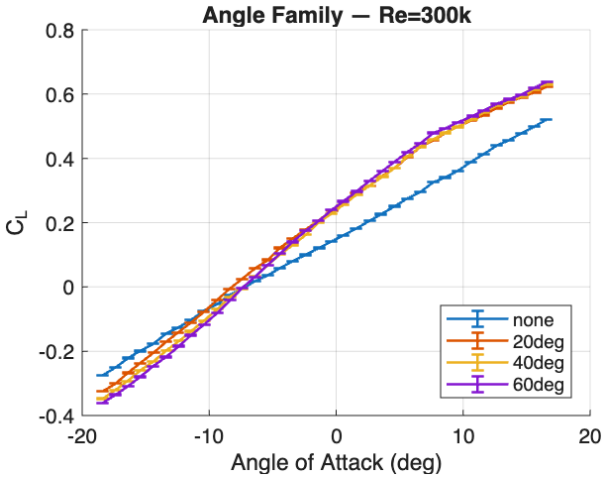

Fig. 4 C_L **vs.** α**, Angle, 300k Re**

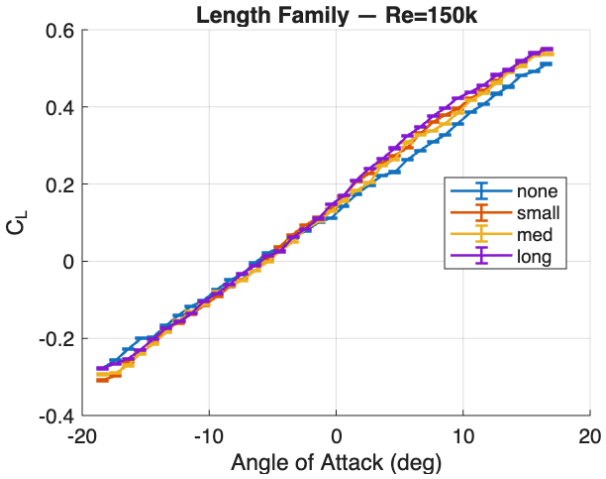

Fig. 5 C_L **vs.** α**, Length, 150k Re**

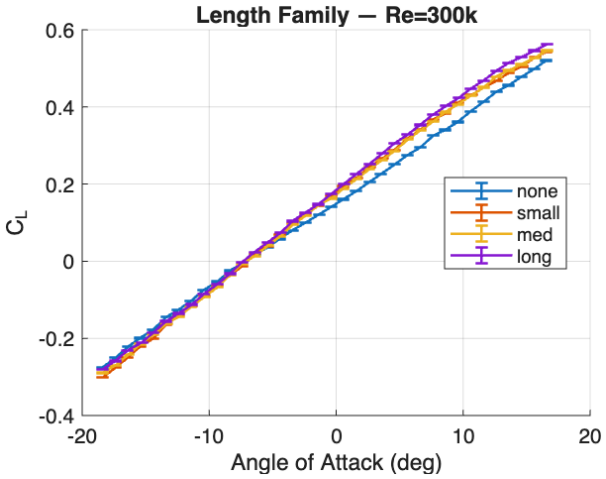

Fig. 6 C_L **vs.** α**, Length, 300k Re**

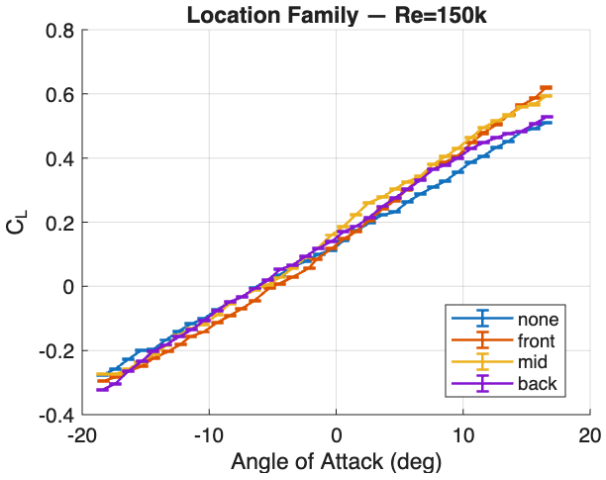

Fig. 7 C_L **vs.** α**, Location, 150k Re**

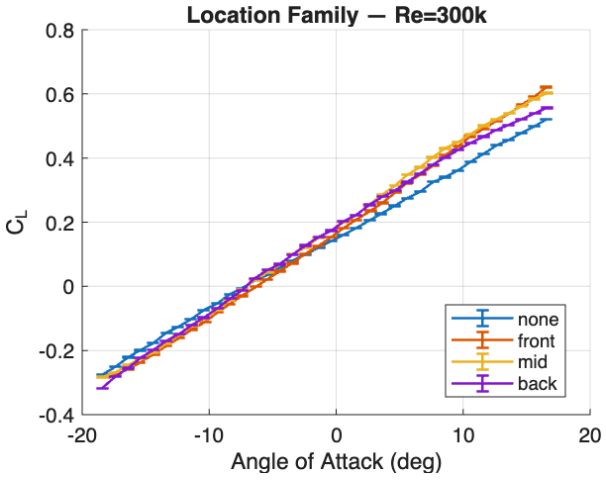

Fig. 8 C_L **vs.** α**, Location, 300k Re**

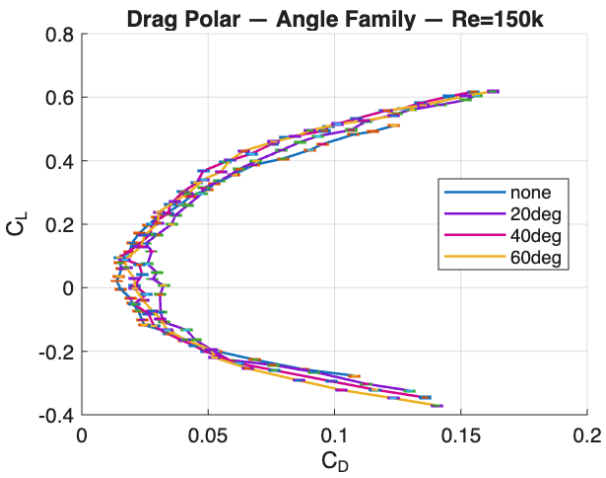

Fig. 9 Drag Polar, Angle, 150k Re

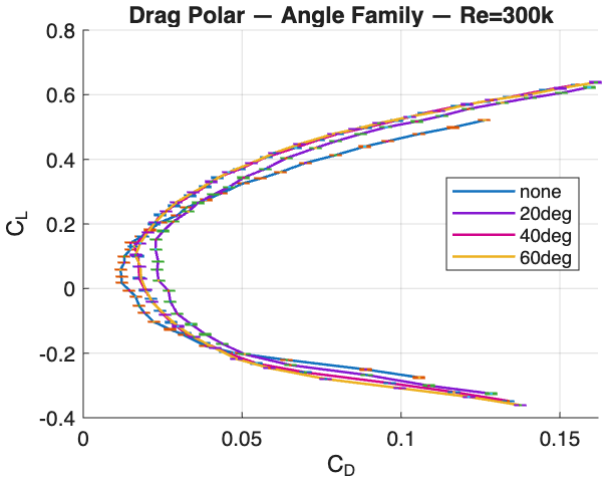

Fig. 10 Drag Polar, Angle, 300k Re

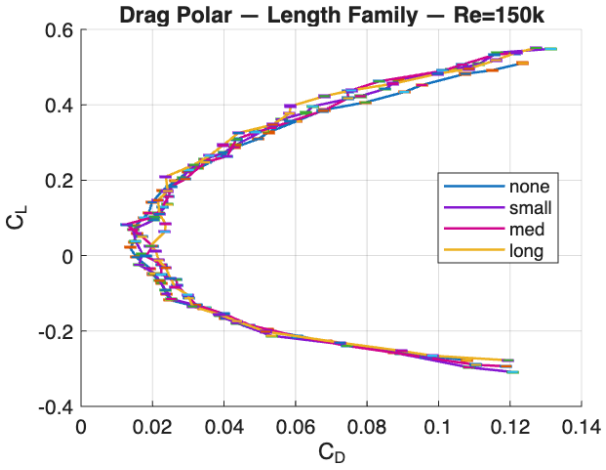

Fig. 11 Drag Polar, Length, 150k Re

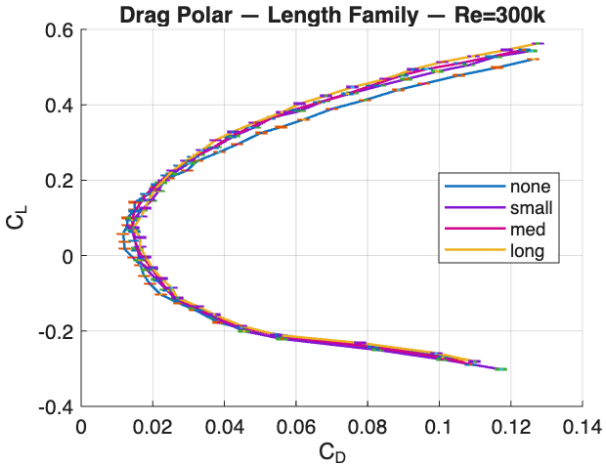

Fig. 12 Drag Polar, Length, 300k Re

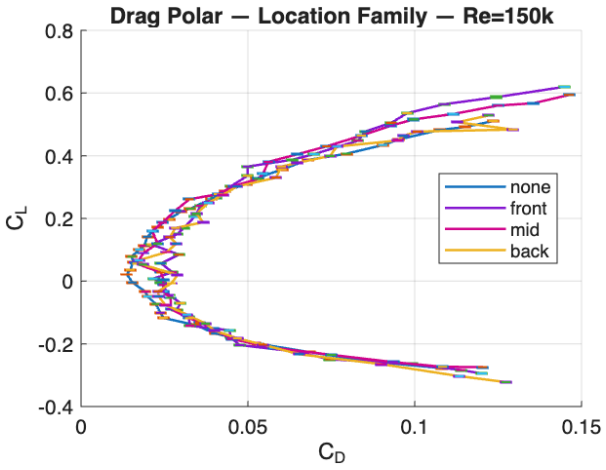

Fig. 13 Drag Polar, Location, 150k Re

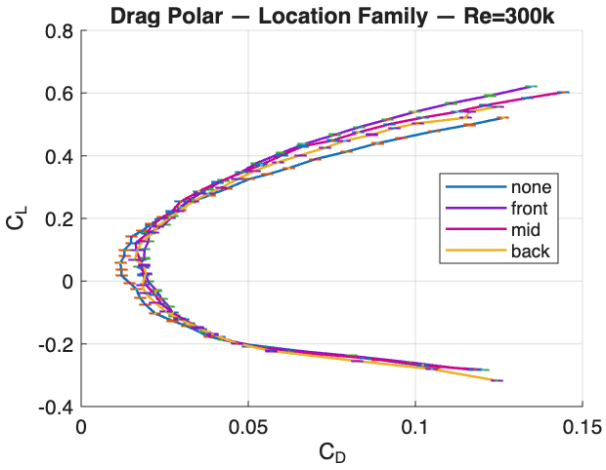

Fig. 14 Drag Polar, Location, 300k Re

Across all three winglet families, all configurations dramatically increase lift compared to the control. In every C_L vs. α plot, the winglet curves sit above the no-winglet curve for the latter half of the linear region. The effect is largest at a higher α because reducing induced drag shrinks downwash, which increases the effective angle of attack, therefore boosting lift.

The results show that different winglet geometries change lift by different amounts. Within the angle family, all subsets increase C_L similarly, though a steeper angle gives slightly more lift. Within the length family, all subsets match the behavior displaying that a longer winglet acts effectively like a larger wingspan, creating an increase in lift relative to the control. Within the location family, a winglet further back produces the greatest lift increase, with a winglet further forward producing the smallest. This aligns with how the circulation distribution interacts with wingtip vortex formation.

For every configuration, increasing the Reynolds number from 150k to 300k increases C_L. This is shown within the plots, where the 300k slope is slightly steeper and the curves shift upward. A higher Reynolds number reduces viscous effects, delays separation, and produces a strong boundary layer, which works to the benefit of the airfoil.

The drag polar show that C_D drops at a Reynolds number of 300k for the same C_L. As shown, the entire curve shifts left. This matches theory, which states that a higher Reynolds number reduces friction drag and delays stall, decreasing induced drag in the moderate range for α.

For every configuration, the stall moves to a higher α at a Reynolds number of 300k. Shown the plots for C_L vs. α, the cuvres start bending sooner at a Reynolds number of 150k. This aligns with theory, since a strong boundary layer at a higher Reynolds number resist separation, resulting in later stall.

The winglet themselves seems to have minimal affect on stall. Between all 3 families, the winglet seem push the stall point slightly higher, though Reynolds number has a much stronger effect. Winglet suppress the wingtip vortex, reducing induced drag and reducing downwash in the further regions. This keeps flow attach for longer, which can be seen on the 'mid' and 'back' locations as well as 'long' winglet length.

Thin airfoil theory predicts that C_L will be close to $2\pi\alpha$, meaning a lift-curve slope of about 6.28 per radian or 0.11 per degree. From the C_L vs. α plots, all configurations show a slope around 0.95-0.105 per degree, which is roughly 5.5-6.0 per radian. This is slightly below the thin-airfoil prediction due to viscous effects and finite-span that are ignored by theory. Nonetheless, the values are relatively close to predictions and display the same behavior in the linear region, which is approximately $\alpha = -12°$ to $\alpha = 12°$. Entering higher angles of attack, thin-airfoil theory begins to implode as flow separation, originating from ignored viscous effects, causes stall.

V. Conclusion

In this experiment the winglet were expected to increase lift by reducing wing-tip vortex strength and weakening the downwash induced on the wing. Across all families, configurations, and Reynolds numbers, the measured data follows this expectation. Every winglet produces a higher lift curve than the control. The increase is consistent across nearly the entire angle of attack range. Winglets shift the C_L vs. α curve upwards without significantly changing the slope. This shows that the wing experiences less induced downwash, which increases the effective angle of attack. The effect becomes stronger at a Reynolds number of 300k, where the boundary layer is stronger and the wing behaves close to ideally.

The winglets were expected to produce a decrease in induced drag at the cost of profile drag from the increases surface area, and the drag polars confirm this. At lower lift values, the differences are small since the profile drag dominates, and all configurations behave similarly. As C_L increase, the control consistently displays higher C_D values compared with every other winglet configuration, especially in the middle region where the induced drag has a much higher contribution.

Angled winglets with small angles were expected to reduce drag, while larger angles were expected to do the same at the cost of an increase in profile drag. The results show that winglet at 20° and 40° perform nearly identical to one another, and consistently better than the control. Winglets at 60° show a slightly higher drag at some points due to an increase in surface area and therefore profile drag, though still showing higher lift than the control.

Longer winglets were expected to give larger reductions in induced drag but create larger increases in profile drag due to their dramatic increase in surface area. In the resulting data, the 'long' configuration consistently yields the best lift increase and lowest induced drag, well outperforming the control. The other two configurations, 'small' and 'med' behave similarly, while still showing an increase lift relative to the control.

Winglet placement was expected to affect on where the vortex is diverted and how flow reattaches. Winglets further back performed best with an overall increase in lift and decrease in drag. Winglet towards the middle are slightly behind it, with a smaller increase in lift and smaller decrease in drag. Contrary, winglets placed towards the front show a higher drag, suggesting a strong, negative influence on pressure distribution towards the leading edge, resulting in drag.

For possible errors, there are many uncertainties that are inherently unavoidable, namely uncertainties from instrumentation like that used in force balance measures, pitch angle measures, and ambient conditions. Additionally, the data collection for this experiment was spread across multiple different lab groups, which introduced variability in data-taking efficiency. Of course, all calculations in this lab were done under standard aerodynamic assumptions, where computational values were done through MATLAB using built-in functions that can create somewhat coarse data. Though numerical values cannot be completely accurate, the patterns for displayed behavior still hold true.

Based on the data, the optimal winglet configuration seems to be long and far back. The highest lift increase across the full range for angles of attack was observed on both, as well as the lowest drag at moderate to high lift values. The drag polars for each display strong, clear reductions in induced drag for the same or greater lift. Additionally, neither show unusual stall behavior or instability that is present with other winglet configurations, as well as much lower drag penalty for the increase in surface area. For low-speed flight with low Reynolds number conditions, induced drag dominates a large portion of the total drag. The best configuration, then, is the one that most effectively reduces induced drag without adding profile drag or other penalties. A long winglet placed further back does exactly this, providing a large reduction in vortex influence, and minimizing penalties.

In aircraft design, experiments like this are exactly what is done to figure out the ideal ways to maximize efficiency, flight range, and fuel consumption along with other considerations. Winglet are a major example of geometric changes to a plane wing that can produce meaningful reductions in drag while improving lift and increasing aerodynamic efficiency. The widespread adoption of winglets on commercial airlines such as the Boeing 737, 757, 767, and personal jets like the Gulfstream V were largely because of experimentation that showed increases in performance and efficiency. Aviation Partners Boeing report that their blended winglet typically yield up to 7.0% reduction in cruising altitude fuel consumption, saving millions annually [32]. This shows that the method of experimentation to demonstrate the effects of various winglet configurations on aerodynamic efficiency goes well beyond the classroom and directly apply to industrial settings.

Appendix A

Table A-1: Density and Uncertainty

Winglet Config	Temperature, °C	Pressure, kPa	Density, ρ	Uncertainty, δ_ρ
None	29.6	96.6	1.1116	0.00385
20deg	29.2	96.6	1.113	0.00386
40deg	27.7	96.6	1.1186	0.00389
60deg	26.9	96.5	1.1204	0.00391
Small	22.1	97.98	1.1561	0.00409
Medium	24.6	96.99	1.1348	0.00399
Long	24.3	97.0	1.1361	0.00399
Front	24.0	97.0	1.1372	0.00400
Middle	29.1	96.9	1.1169	0.00387
Back	29.6	96.8	1.1139	0.00385

Table A-2: C_L vs. α Plot Data

Table 1: G8, none, 150k Re

α deg	C_L	dC_L
-18.416	-0.2773	0.00152
-17.367	-0.2568	0.00149
-16.348	-0.2268	0.00145
-15.349	-0.1998	0.00142
-14.411	-0.1966	0.00142
-13.409	-0.1672	0.00139
-12.416	-0.14	0.00136
-11.445	-0.1173	0.00135
-10.427	-0.101	0.00134
-9.373	-0.0729	0.00132
-8.365	-0.049	0.00131
-7.41	-0.0337	0.00131
-6.407	-0.0043	0.00131
-5.398	0.0212	0.00131
-4.434	0.0362	0.00131
-3.436	0.0598	0.00132
-2.415	0.0782	0.00133
-1.35	0.1009	0.00134
-0.356	0.1127	0.00134
0.552	0.1416	0.00137
1.586	0.1732	0.00139
2.625	0.1978	0.00142
3.604	0.2223	0.00145
4.637	0.2311	0.00146
5.597	0.2628	0.0015
6.619	0.2872	0.00153
7.627	0.3093	0.00157
8.559	0.3269	0.00159
9.569	0.3566	0.00164
10.607	0.3866	0.00169
11.602	0.4065	0.00173
12.632	0.4339	0.00178
13.576	0.4522	0.00182
14.6	0.4823	0.00188
15.622	0.4916	0.00189
16.554	0.5107	0.00193

Table 2: G8, none, 300k Re

α deg	CL	dCL
-18.415	-0.2754	0.00039
-17.367	-0.2505	0.00038
-16.366	-0.2209	0.00037
-15.443	-0.1992	0.00036
-14.415	-0.1775	0.00035
-13.371	-0.1446	0.00034
-12.446	-0.1265	0.00034
-11.448	-0.1033	0.00034
-10.418	-0.0742	0.00033
-9.353	-0.0532	0.00033
-8.378	-0.0247	0.00033
-7.416	-0.0057	0.00033
-6.401	0.0175	0.00033
-5.38	0.0365	0.00033
-4.443	0.0579	0.00033
-3.436	0.0803	0.00033
-2.416	0.0999	0.00033
-1.338	0.1215	0.00034
-0.363	0.1413	0.00034
0.557	0.1604	0.00035
1.589	0.1815	0.00035
2.618	0.2055	0.00036
3.541	0.2262	0.00036
4.612	0.2509	0.00037
5.58	0.2746	0.00038
6.621	0.2947	0.00039
7.63	0.3254	0.0004
8.589	0.3406	0.00041
9.572	0.3608	0.00042
10.599	0.3887	0.00043
11.597	0.4128	0.00044
12.638	0.4398	0.00045
13.578	0.4558	0.00046
14.604	0.4782	0.00048
15.616	0.4987	0.00049
16.562	0.5208	0.0005

Table 3: G8, 20 deg, 150k Re

α deg	CL	dCL
-18.399	-0.324	0.0016
-17.256	-0.3025	0.00157
-16.346	-0.2649	0.00151
-15.409	-0.2434	0.00148
-14.411	-0.2274	0.00146
-13.393	-0.1936	0.00142
-12.443	-0.1638	0.00139
-11.436	-0.1334	0.00137
-10.42	-0.1078	0.00135
-9.364	-0.0779	0.00133
-8.348	-0.022	0.00132
-7.413	0.0072	0.00132
-6.397	0.0273	0.00132
-5.375	0.0482	0.00132
-4.426	0.0746	0.00133
-3.431	0.1147	0.00135
-2.41	0.1395	0.00137
-1.37	0.1666	0.0014
-0.358	0.1992	0.00143
0.599	0.2292	0.00146
1.596	0.2602	0.0015
2.633	0.295	0.00155
3.666	0.3137	0.00158
4.557	0.3359	0.00162
5.606	0.373	0.00168
6.629	0.3988	0.00173
7.639	0.4333	0.00179
8.6	0.4592	0.00184
9.582	0.4771	0.00188
10.613	0.4969	0.00192
11.616	0.5234	0.00197
12.57	0.5473	0.00202
13.578	0.5603	0.00205
14.616	0.5766	0.00209
15.648	0.5911	0.00212
16.556	0.6055	0.00215

Table 4: G8, 20 deg, 300k Re

α deg	CL	dCL
-18.408	-0.3255	0.00042
-17.371	-0.3006	0.0004
-16.412	-0.2675	0.00039
-15.439	-0.2371	0.00037
-14.347	-0.2036	0.00036
-13.377	-0.1704	0.00035
-12.452	-0.1417	0.00035
-11.433	-0.1109	0.00034
-10.424	-0.0783	0.00033
-9.358	-0.0403	0.00033
-8.443	-0.0072	0.00033
-7.408	0.0248	0.00033
-6.394	0.0576	0.00033
-5.378	0.084	0.00033
-4.428	0.1214	0.00034
-3.423	0.1508	0.00035
-2.411	0.1784	0.00035
-1.37	0.2072	0.00036
-0.335	0.238	0.00037
0.578	0.2649	0.00038
1.598	0.2914	0.00039
2.636	0.3146	0.0004
3.557	0.3434	0.00041
4.638	0.3705	0.00042
5.605	0.4032	0.00044
6.638	0.4351	0.00045
7.672	0.4561	0.00046
8.576	0.4784	0.00048
9.601	0.4992	0.00049
10.615	0.5173	0.0005
11.619	0.5345	0.00051
12.625	0.5559	0.00052
13.602	0.5753	0.00053
14.622	0.5904	0.00054
15.641	0.6055	0.00055
16.597	0.6229	0.00056

Table 5: G8, 40 deg, 150k Re

α deg	C_L	dC_L
-18.39	-0.3456	0.00166
-17.355	-0.321	0.00161
-16.421	-0.2948	0.00157
-15.435	-0.26	0.00152
-14.398	-0.238	0.00149
-13.393	-0.2019	0.00145
-12.389	-0.1835	0.00143
-11.431	-0.1465	0.00139
-10.417	-0.1206	0.00137
-9.358	-0.0821	0.00135
-8.341	-0.0523	0.00134
-7.41	-0.0213	0.00133
-6.416	0.0067	0.00133
-5.368	0.0406	0.00133
-4.429	0.0723	0.00135
-3.421	0.0952	0.00136
-2.397	0.1314	0.00138
-1.364	0.1692	0.00141
-0.402	0.2013	0.00145
0.621	0.2354	0.00149
1.603	0.2626	0.00152
2.635	0.3019	0.00158
3.55	0.3303	0.00163
4.562	0.3677	0.00169
5.618	0.3956	0.00174
6.638	0.4215	0.00179
7.606	0.453	0.00185
8.581	0.4733	0.00189
9.59	0.494	0.00193
10.608	0.5088	0.00196
11.612	0.5319	0.00201
12.609	0.5565	0.00206
13.594	0.5646	0.00208
14.621	0.582	0.00212
15.635	0.6022	0.00217
16.553	0.6173	0.0022

Table 6: G8, 40 deg, 300k Re

α deg	C_L	dC_L
-18.4	-0.348	0.00043
-17.389	-0.3205	0.00042
-16.428	-0.2927	0.0004
-15.424	-0.2597	0.00038
-14.391	-0.2322	0.00037
-13.363	-0.1973	0.00036
-12.331	-0.1672	0.00035
-11.435	-0.1379	0.00035
-10.4	-0.1047	0.00034
-9.349	-0.0689	0.00034
-8.381	-0.0318	0.00033
-7.426	-0.0049	0.00033
-6.388	0.0319	0.00033
-5.359	0.0683	0.00034
-4.442	0.1005	0.00034
-3.416	0.1304	0.00035
-2.394	0.1618	0.00035
-1.407	0.2002	0.00036
-0.374	0.2277	0.00037
0.582	0.256	0.00038
1.609	0.2872	0.00039
2.608	0.3146	0.0004
3.658	0.3433	0.00041
4.576	0.3691	0.00043
5.624	0.4063	0.00044
6.643	0.4358	0.00046
7.652	0.4599	0.00047
8.562	0.479	0.00048
9.588	0.4981	0.00049
10.657	0.5204	0.0005
11.622	0.5428	0.00052
12.637	0.5643	0.00053
13.598	0.5785	0.00054
14.62	0.5924	0.00055
15.584	0.6143	0.00056
16.574	0.6308	0.00057

Table 7: G8, 60 deg, 150k Re

α deg	C_L	dC_L
-18.4	-0.3706	0.00171
-17.35	-0.348	0.00167
-16.367	-0.322	0.00163
-15.435	-0.2919	0.00158
-14.39	-0.2538	0.00152
-13.374	-0.2198	0.00148
-12.471	-0.1961	0.00145
-11.338	-0.163	0.00142
-10.41	-0.1337	0.00139
-9.355	-0.0992	0.00137
-8.376	-0.0723	0.00136
-7.405	-0.0402	0.00134
-6.392	-0.0021	0.00134
-5.377	0.0281	0.00134
-4.374	0.0639	0.00135
-3.423	0.088	0.00136
-2.401	0.1296	0.00139
-1.453	0.1648	0.00142
-0.415	0.203	0.00146
0.626	0.2381	0.0015
1.606	0.273	0.00155
2.625	0.296	0.00158
3.583	0.3407	0.00166
4.644	0.3649	0.0017
5.753	0.401	0.00176
6.638	0.4307	0.00182
7.648	0.4596	0.00187
8.592	0.4761	0.00191
9.587	0.4949	0.00195
10.595	0.5153	0.00199
11.607	0.5262	0.00201
12.585	0.5413	0.00205
13.602	0.5579	0.00208
14.616	0.5745	0.00212
15.636	0.6043	0.00219
16.57	0.6182	0.00222

Table 8: G8, 60 deg, 300k Re

α deg	C_L	dC_L
-18.411	-0.3612	0.00044
-17.356	-0.3352	0.00042
-16.39	-0.3086	0.00041
-15.436	-0.28	0.0004
-14.404	-0.2462	0.00038
-13.402	-0.218	0.00037
-12.373	-0.1843	0.00036
-11.433	-0.1502	0.00035
-10.405	-0.1171	0.00035
-9.358	-0.0809	0.00034
-8.334	-0.0415	0.00034
-7.413	-0.0033	0.00034
-6.393	0.0314	0.00034
-5.413	0.0681	0.00034
-4.412	0.1035	0.00034
-3.422	0.1402	0.00035
-2.401	0.1743	0.00036
-1.365	0.2051	0.00037
-0.361	0.2393	0.00038
0.565	0.2664	0.00039
1.605	0.2972	0.0004
2.635	0.3305	0.00041
3.636	0.3603	0.00042
4.566	0.3884	0.00044
5.616	0.4197	0.00045
6.64	0.4468	0.00047
7.649	0.4788	0.00048
8.58	0.4928	0.00049
9.581	0.5119	0.0005
10.746	0.5316	0.00051
11.614	0.5491	0.00052
12.656	0.5696	0.00054
13.631	0.5836	0.00055
14.611	0.5988	0.00056
15.63	0.62	0.00057
16.572	0.6379	0.00058

Table 9: G8, small, 150k Re

α deg	C_L	dC_L
-18.399	-0.3088	0.0017
-17.355	-0.2965	0.00168
-16.36	-0.2609	0.00163
-15.428	-0.24	0.0016
-14.409	-0.2125	0.00156
-13.406	-0.1792	0.00152
-12.429	-0.1596	0.0015
-11.438	-0.138	0.00148
-10.417	-0.1152	0.00146
-9.356	-0.091	0.00145
-8.41	-0.0666	0.00143
-7.404	-0.0474	0.00143
-6.394	-0.0245	0.00142
-5.375	0.0053	0.00142
-4.435	0.0379	0.00143
-3.452	0.0685	0.00144
-2.401	0.0942	0.00145
-1.366	0.1131	0.00146
-0.39	0.1352	0.00148
0.571	0.1691	0.00151
1.602	0.206	0.00155
2.595	0.2273	0.00158
3.659	0.2551	0.00162
4.565	0.2733	0.00164
5.587	0.2935	0.00168
6.63	0.331	0.00174
7.649	0.3613	0.00179
8.554	0.3789	0.00183
9.579	0.3959	0.00186
10.627	0.4229	0.00191
11.645	0.4426	0.00195
12.636	0.4669	0.002
13.592	0.4925	0.00206
14.612	0.5082	0.00209
15.646	0.5382	0.00216
16.555	0.5483	0.00219

Table 10: G8, small, 300k Re

α deg	C_L	dC_L
-18.398	-0.3018	0.00043
-17.36	-0.2754	0.00042
-16.426	-0.2501	0.00041
-15.431	-0.221	0.00039
-14.398	-0.2004	0.00039
-13.412	-0.165	0.00038
-12.413	-0.1402	0.00037
-11.352	-0.115	0.00037
-10.408	-0.0899	0.00036
-9.355	-0.0635	0.00036
-8.377	-0.0371	0.00036
-7.39	-0.0126	0.00035
-6.393	0.02	0.00035
-5.404	0.0392	0.00036
-4.441	0.0676	0.00036
-3.425	0.0971	0.00036
-2.4	0.1205	0.00037
-1.365	0.1453	0.00037
-0.354	0.1708	0.00038
0.576	0.1936	0.00038
1.603	0.2164	0.00039
2.64	0.2448	0.0004
3.642	0.2666	0.00041
4.564	0.2885	0.00042
5.608	0.3173	0.00043
6.635	0.3403	0.00044
7.641	0.3674	0.00045
8.595	0.3829	0.00046
9.59	0.4102	0.00047
10.666	0.4311	0.00049
11.615	0.4502	0.0005
12.644	0.4681	0.00051
13.601	0.4883	0.00052
14.621	0.5054	0.00053
15.647	0.528	0.00054
16.556	0.5429	0.00055

Table 11: G8, med, 150k Re

α deg	C_L	dC_L
-18.403	-0.2935	0.00162
-17.358	-0.29	0.00161
-16.405	-0.2702	0.00158
-15.438	-0.2394	0.00154
-14.396	-0.2147	0.00151
-13.379	-0.1843	0.00147
-12.38	-0.1545	0.00144
-11.431	-0.1308	0.00142
-10.403	-0.1129	0.00141
-9.36	-0.079	0.00139
-8.366	-0.0641	0.00138
-7.421	-0.0505	0.00138
-6.389	-0.024	0.00137
-5.392	-0.0017	0.00137
-4.433	0.0258	0.00137
-3.425	0.0499	0.00138
-2.412	0.083	0.00139
-1.363	0.1031	0.0014
-0.402	0.1296	0.00142
0.558	0.1565	0.00145
1.589	0.1831	0.00147
2.647	0.2032	0.00149
3.555	0.2473	0.00155
4.559	0.2635	0.00157
5.605	0.3086	0.00164
6.629	0.3271	0.00167
7.592	0.3386	0.00169
8.562	0.3562	0.00172
9.58	0.3841	0.00177
10.59	0.4172	0.00183
11.613	0.4351	0.00187
12.638	0.4622	0.00192
13.598	0.49	0.00198
14.616	0.5063	0.00202
15.635	0.5328	0.00208
16.684	0.5372	0.00209

Table 12: G8, med, 300k Re

α deg	C_L	dC_L
-18.409	-0.2891	0.00041
-17.359	-0.2699	0.0004
-16.358	-0.242	0.00039
-15.436	-0.2147	0.00038
-14.405	-0.1908	0.00037
-13.362	-0.1617	0.00036
-12.376	-0.1439	0.00036
-11.437	-0.1184	0.00035
-10.406	-0.0932	0.00035
-9.336	-0.0672	0.00035
-8.369	-0.0355	0.00034
-7.423	-0.0064	0.00034
-6.398	0.0134	0.00034
-5.379	0.0399	0.00034
-4.435	0.0637	0.00035
-3.43	0.0942	0.00035
-2.407	0.1178	0.00035
-1.371	0.1461	0.00036
-0.356	0.1629	0.00036
0.565	0.1883	0.00037
1.594	0.2127	0.00038
2.601	0.2381	0.00038
3.625	0.2625	0.00039
4.561	0.285	0.0004
5.651	0.3152	0.00041
6.629	0.339	0.00042
7.654	0.3624	0.00043
8.568	0.3865	0.00045
9.575	0.4065	0.00046
10.629	0.4293	0.00047
11.638	0.4507	0.00048
12.593	0.4785	0.0005
13.586	0.4946	0.0005
14.599	0.5104	0.00051
15.647	0.5275	0.00052
16.583	0.546	0.00054

Table 13: G8, long, 150k Re

α deg	C_L	dC_L
-18.44	-0.2777	0.00159
-17.391	-0.2656	0.00158
-16.399	-0.2528	0.00156
-15.435	-0.2309	0.00153
-14.432	-0.2016	0.00149
-13.404	-0.1742	0.00146
-12.351	-0.1562	0.00144
-11.355	-0.1351	0.00142
-10.426	-0.1036	0.0014
-9.391	-0.084	0.00139
-8.383	-0.0604	0.00138
-7.43	-0.0324	0.00137
-6.427	-0.0126	0.00137
-5.409	0.0131	0.00137
-4.421	0.0255	0.00137
-3.367	0.0631	0.00138
-2.435	0.0839	0.00139
-1.395	0.1102	0.00141
-0.369	0.147	0.00143
0.629	0.1712	0.00146
1.57	0.2094	0.0015
2.625	0.2409	0.00154
3.629	0.2649	0.00157
4.615	0.2928	0.00161
5.608	0.3252	0.00167
6.606	0.3473	0.0017
7.648	0.377	0.00176
8.551	0.3962	0.00179
9.553	0.4228	0.00184
10.568	0.4383	0.00187
11.573	0.4559	0.00191
12.634	0.4824	0.00196
13.567	0.4955	0.00199
14.581	0.5186	0.00204
15.619	0.5388	0.00209
16.641	0.5506	0.00211

Table 14: G8, long, 300k Re

α deg	C_L	dC_L
-18.428	-0.2811	0.00041
-17.391	-0.2586	0.0004
-16.436	-0.2317	0.00039
-15.308	-0.2106	0.00038
-14.422	-0.1857	0.00037
-13.404	-0.1561	0.00036
-12.393	-0.1349	0.00036
-11.347	-0.1122	0.00035
-10.435	-0.0852	0.00035
-9.389	-0.0603	0.00035
-8.365	-0.0324	0.00034
-7.445	-0.0033	0.00034
-6.428	0.0237	0.00034
-5.41	0.0485	0.00035
-4.359	0.074	0.00035
-3.442	0.1039	0.00035
-2.436	0.1258	0.00036
-1.403	0.1476	0.00036
-0.369	0.1749	0.00037
0.594	0.2	0.00037
1.563	0.2252	0.00038
2.619	0.252	0.00039
3.635	0.2792	0.0004
4.609	0.3061	0.00041
5.632	0.3283	0.00042
6.595	0.3529	0.00043
7.621	0.3801	0.00044
8.676	0.4031	0.00046
9.686	0.424	0.00047
10.566	0.4467	0.00048
11.609	0.4684	0.00049
12.632	0.4941	0.0005
13.571	0.5139	0.00052
14.578	0.529	0.00053
15.602	0.5456	0.00054
16.624	0.5627	0.00055

Table 15: G8, front, 150k Re

α deg	C_L	dC_L
-18.287	-0.2947	0.00163
-17.401	-0.2836	0.00161
-16.362	-0.2646	0.00159
-15.304	-0.2492	0.00156
-14.37	-0.2242	0.00153
-13.262	-0.2039	0.0015
-12.252	-0.1808	0.00148
-11.496	-0.1566	0.00146
-10.436	-0.1425	0.00144
-9.379	-0.1129	0.00142
-8.378	-0.0919	0.00141
-7.458	-0.0701	0.0014
-6.424	-0.0441	0.00139
-5.249	-0.0048	0.00138
-4.477	0.0082	0.00138
-3.44	0.0283	0.00138
-2.141	0.0569	0.00139
-1.549	0.0844	0.0014
-0.366	0.1173	0.00142
0.629	0.1491	0.00145
1.559	0.1703	0.00147
2.58	0.2048	0.00151
3.636	0.2404	0.00155
4.583	0.2663	0.00159
5.573	0.3019	0.00164
6.599	0.3363	0.0017
7.638	0.3654	0.00175
8.599	0.3871	0.00179
9.548	0.4052	0.00182
10.672	0.448	0.00191
11.577	0.4775	0.00197
12.643	0.505	0.00203
13.672	0.5357	0.00209
14.578	0.5644	0.00216
15.639	0.5866	0.00221
16.519	0.62	0.00229

Table 16: G8, front, 300k Re

α deg	C_L	dC_L
-18.278	-0.2825	0.00041
-17.399	-0.277	0.00041
-16.372	-0.2577	0.0004
-15.478	-0.2385	0.00039
-14.38	-0.2119	0.00038
-13.406	-0.1866	0.00037
-12.371	-0.1614	0.00037
-11.37	-0.1346	0.00036
-10.293	-0.1106	0.00035
-9.365	-0.0816	0.00035
-8.384	-0.0553	0.00035
-7.446	-0.0298	0.00035
-6.31	-0.0014	0.00034
-5.423	0.0222	0.00034
-4.429	0.0471	0.00035
-3.467	0.0723	0.00035
-2.428	0.1011	0.00035
-1.392	0.1263	0.00036
-0.379	0.1537	0.00036
0.534	0.1805	0.00037
1.565	0.2072	0.00038
2.728	0.2358	0.00039
3.632	0.26	0.00039
4.686	0.2934	0.00041
5.514	0.3209	0.00042
6.601	0.3475	0.00043
7.623	0.3764	0.00044
8.579	0.409	0.00046
9.64	0.4367	0.00047
10.548	0.4672	0.00049
11.607	0.4908	0.0005
12.625	0.5158	0.00052
13.662	0.5395	0.00053
14.659	0.5673	0.00055
15.631	0.5916	0.00056
16.568	0.6211	0.00058

Table 17: G8, mid, 150k Re

α deg	C_L	dC_L
-18.428	-0.2743	0.00153
-17.338	-0.2733	0.00153
-16.386	-0.2583	0.00151
-15.436	-0.2351	0.00148
-14.347	-0.2129	0.00145
-13.397	-0.1846	0.00142
-12.365	-0.1517	0.00139
-11.401	-0.1313	0.00137
-10.434	-0.1182	0.00136
-9.374	-0.0891	0.00134
-8.361	-0.0535	0.00133
-7.434	-0.032	0.00132
-6.406	-0.012	0.00132
-5.41	0.0044	0.00132
-4.447	0.0274	0.00132
-3.442	0.0557	0.00133
-2.421	0.0898	0.00134
-1.442	0.1196	0.00136
-0.371	0.16	0.00139
0.575	0.1864	0.00142
1.583	0.2244	0.00146
2.578	0.261	0.00151
3.648	0.2778	0.00153
4.64	0.304	0.00157
5.595	0.3261	0.00161
6.613	0.3423	0.00163
7.642	0.3805	0.0017
8.593	0.4041	0.00174
9.56	0.4302	0.00179
10.64	0.4642	0.00185
11.602	0.4953	0.00192
12.65	0.5159	0.00196
13.582	0.5332	0.002
14.671	0.5601	0.00205
15.632	0.5675	0.00207
16.564	0.5939	0.00213

Table 18: G8, mid, 300k Re

α deg	C_L	dC_L
-18.425	-0.2831	0.0004
-17.378	-0.2679	0.00039
-16.349	-0.2458	0.00038
-15.423	-0.2242	0.00037
-14.407	-0.2074	0.00036
-13.403	-0.179	0.00035
-12.386	-0.1525	0.00035
-11.324	-0.1222	0.00034
-10.419	-0.1007	0.00034
-9.362	-0.0731	0.00033
-8.409	-0.0438	0.00033
-7.435	-0.0108	0.00033
-6.405	0.0199	0.00033
-5.387	0.044	0.00033
-4.404	0.0676	0.00033
-3.439	0.0998	0.00034
-2.416	0.1214	0.00034
-1.378	0.1523	0.00035
-0.365	0.1757	0.00035
0.566	0.1989	0.00036
1.589	0.222	0.00037
2.582	0.2541	0.00038
3.643	0.286	0.00039
4.666	0.3148	0.0004
5.595	0.3476	0.00041
6.622	0.3714	0.00042
7.599	0.402	0.00044
8.573	0.4301	0.00045
9.57	0.4491	0.00046
10.586	0.4743	0.00047
11.603	0.5009	0.00049
12.649	0.5217	0.0005
13.608	0.5402	0.00051
14.597	0.5609	0.00052
15.568	0.5845	0.00054
16.617	0.6024	0.00055

Table 19: G8, back, 150k Re

α deg	C_L	dC_L
-18.418	-0.3222	0.0016
-17.378	-0.3032	0.00157
-16.374	-0.2648	0.00151
-15.298	-0.2332	0.00147
-14.422	-0.2027	0.00143
-13.411	-0.1825	0.00141
-12.382	-0.1576	0.00139
-11.395	-0.1354	0.00137
-10.395	-0.1069	0.00135
-9.372	-0.0755	0.00133
-8.373	-0.0485	0.00132
-7.418	-0.0323	0.00132
-6.417	-0.0068	0.00131
-5.358	0.0194	0.00131
-4.428	0.0528	0.00132
-3.442	0.0664	0.00133
-2.433	0.0927	0.00134
-1.38	0.1195	0.00136
-0.354	0.1401	0.00137
0.576	0.1698	0.0014
1.587	0.1876	0.00141
2.617	0.2151	0.00144
3.647	0.2494	0.00149
4.644	0.2759	0.00152
5.596	0.3019	0.00156
6.608	0.3301	0.00161
7.641	0.3654	0.00166
8.554	0.3773	0.00169
9.562	0.3993	0.00172
10.606	0.4291	0.00178
11.626	0.4485	0.00182
12.646	0.4633	0.00185
13.604	0.4771	0.00187
14.598	0.4834	0.00189
15.64	0.5068	0.00193
16.574	0.5286	0.00198

Table 20: G8, back, 300k Re

α deg	C_L	dC_L
-18.43	-0.3172	0.00041
-17.373	-0.2808	0.00039
-16.382	-0.2548	0.00038
-15.404	-0.2229	0.00037
-14.417	-0.1988	0.00036
-13.376	-0.1702	0.00035
-12.346	-0.1483	0.00034
-11.359	-0.1205	0.00034
-10.429	-0.0976	0.00034
-9.374	-0.0691	0.00033
-8.355	-0.0384	0.00033
-7.442	-0.0128	0.00033
-6.409	0.0253	0.00033
-5.414	0.0507	0.00033
-4.455	0.069	0.00033
-3.443	0.0988	0.00033
-2.425	0.1273	0.00034
-1.348	0.1543	0.00035
-0.36	0.1737	0.00035
0.581	0.2027	0.00036
1.583	0.2227	0.00036
2.628	0.254	0.00037
3.649	0.2795	0.00038
4.643	0.2991	0.00039
5.607	0.3248	0.0004
6.616	0.3519	0.00041
7.618	0.3792	0.00042
8.566	0.4014	0.00043
9.616	0.4252	0.00045
10.601	0.4474	0.00046
11.627	0.467	0.00047
12.627	0.4878	0.00048
13.582	0.5034	0.00049
14.601	0.521	0.0005
15.643	0.5397	0.00051
16.599	0.5566	0.00052

Table A-3: C_L vs. C_D Plot Data

Table 1: G8, none, 150k Re

C_D	C_L	dC_D	dC_L
0.108	-0.2773	0.00136	0.00152
0.0875	-0.2568	0.00135	0.00149
0.0685	-0.2268	0.00134	0.00145
0.0532	-0.1998	0.00133	0.00142
0.0521	-0.1966	0.00133	0.00142
0.0403	-0.1672	0.00132	0.00139
0.0343	-0.14	0.00132	0.00136
0.0247	-0.1173	0.00131	0.00135
0.0238	-0.101	0.00131	0.00134
0.0224	-0.0729	0.00131	0.00132
0.0199	-0.049	0.00131	0.00131
0.0193	-0.0337	0.00131	0.00131
0.0154	-0.0043	0.00131	0.00131
0.0137	0.0212	0.00131	0.00131
0.0147	0.0362	0.00131	0.00131
0.0156	0.0598	0.00131	0.00132
0.0152	0.0782	0.00131	0.00133
0.0175	0.1009	0.00131	0.00134
0.0189	0.1127	0.00131	0.00134
0.0199	0.1416	0.00131	0.00137
0.0228	0.1732	0.00132	0.00139
0.0264	0.1978	0.00132	0.00142
0.03	0.2223	0.00132	0.00145
0.0327	0.2311	0.00133	0.00146
0.0392	0.2628	0.00133	0.0015
0.043	0.2872	0.00134	0.00153
0.0496	0.3093	0.00134	0.00157
0.0524	0.3269	0.00135	0.00159
0.0603	0.3566	0.00135	0.00164
0.068	0.3866	0.00136	0.00169
0.0796	0.4065	0.00137	0.00173
0.0904	0.4339	0.00138	0.00178
0.0953	0.4522	0.00139	0.00182
0.1075	0.4823	0.00141	0.00188
0.115	0.4916	0.00141	0.00189
0.1236	0.5107	0.00142	0.00193

Table 2: G8, none, 300k Re

CD	CL	dCD	dCL
0.1058	-0.2754	0.00041	0.00039
0.0889	-0.2505	0.0004	0.00038
0.064	-0.2209	0.00038	0.00037
0.0474	-0.1992	0.00037	0.00036
0.0384	-0.1775	0.00036	0.00035
0.0318	-0.1446	0.00035	0.00034
0.0273	-0.1265	0.00035	0.00034
0.0222	-0.1033	0.00034	0.00034
0.0191	-0.0742	0.00033	0.00033
0.0176	-0.0532	0.00033	0.00033
0.0165	-0.0247	0.00033	0.00033
0.0145	-0.0057	0.00033	0.00033
0.0121	0.0175	0.00033	0.00033
0.012	0.0365	0.00033	0.00033
0.0117	0.0579	0.00033	0.00033
0.0129	0.0803	0.00033	0.00033
0.0129	0.0999	0.00034	0.00033
0.0149	0.1215	0.00034	0.00034
0.015	0.1413	0.00035	0.00034
0.0183	0.1604	0.00036	0.00035
0.0209	0.1815	0.00036	0.00035
0.0243	0.2055	0.00037	0.00036
0.0296	0.2262	0.00038	0.00036
0.0325	0.2509	0.00039	0.00037
0.0385	0.2746	0.00041	0.00038
0.0435	0.2947	0.00042	0.00039
0.0502	0.3254	0.00043	0.0004
0.0558	0.3406	0.00044	0.00041
0.0622	0.3608	0.00046	0.00042
0.0699	0.3887	0.00047	0.00043
0.0794	0.4128	0.00049	0.00044
0.0886	0.4398	0.00051	0.00045
0.0957	0.4558	0.00052	0.00046
0.1056	0.4782	0.00054	0.00048
0.1162	0.4987	0.00055	0.00049
0.1262	0.5208	0.00057	0.0005

Table 3: G8, 20 deg, 150k Re

C_D	C_L	dC_D	dC_L
0.1296	-0.324	0.00139	0.0016
0.1124	-0.3025	0.00138	0.00157
0.0919	-0.2649	0.00136	0.00151
0.0757	-0.2434	0.00135	0.00148
0.0582	-0.2274	0.00134	0.00146
0.0509	-0.1936	0.00133	0.00142
0.0449	-0.1638	0.00133	0.00139
0.0415	-0.1334	0.00133	0.00137
0.0324	-0.1078	0.00132	0.00135
0.0312	-0.0779	0.00132	0.00133
0.0309	-0.022	0.00132	0.00132
0.0324	0.0072	0.00132	0.00132
0.028	0.0273	0.00132	0.00132
0.0298	0.0482	0.00132	0.00132
0.026	0.0746	0.00132	0.00133
0.0277	0.1147	0.00132	0.00135
0.0253	0.1395	0.00132	0.00137
0.0297	0.1666	0.00133	0.0014
0.0355	0.1992	0.00133	0.00143
0.0371	0.2292	0.00133	0.00146
0.042	0.2602	0.00134	0.0015
0.0472	0.295	0.00135	0.00155
0.0481	0.3137	0.00135	0.00158
0.0546	0.3359	0.00136	0.00162
0.0623	0.373	0.00137	0.00168
0.0689	0.3988	0.00137	0.00173
0.0791	0.4333	0.00139	0.00179
0.0865	0.4592	0.0014	0.00184
0.0934	0.4771	0.0014	0.00188
0.1065	0.4969	0.00142	0.00192
0.1123	0.5234	0.00143	0.00197
0.1245	0.5473	0.00144	0.00202
0.1302	0.5603	0.00145	0.00205
0.1421	0.5766	0.00146	0.00209
0.152	0.5911	0.00148	0.00212
0.156	0.6055	0.00148	0.00215

Table 4: G8, 20 deg, 300k Re

C_D	C_L	dC_D	dC_L
0.1284	-0.3255	0.00044	0.00042
0.1087	-0.3006	0.00043	0.0004
0.0891	-0.2675	0.00041	0.00039
0.0652	-0.2371	0.00039	0.00037
0.0508	-0.2036	0.00038	0.00036
0.0437	-0.1704	0.00036	0.00035
0.0385	-0.1417	0.00035	0.00035
0.034	-0.1109	0.00034	0.00034
0.0296	-0.0783	0.00034	0.00033
0.0274	-0.0403	0.00033	0.00033
0.0269	-0.0072	0.00033	0.00033
0.0237	0.0248	0.00033	0.00033
0.0232	0.0576	0.00033	0.00033
0.0236	0.084	0.00034	0.00033
0.0228	0.1214	0.00035	0.00034
0.0228	0.1508	0.00035	0.00035
0.0252	0.1784	0.00036	0.00035
0.0283	0.2072	0.00038	0.00036
0.0331	0.238	0.00039	0.00037
0.0361	0.2649	0.0004	0.00038
0.041	0.2914	0.00042	0.00039
0.046	0.3146	0.00043	0.0004
0.0505	0.3434	0.00045	0.00041
0.0574	0.3705	0.00046	0.00042
0.0638	0.4032	0.00048	0.00044
0.073	0.4351	0.0005	0.00045
0.0796	0.4561	0.00052	0.00046
0.0873	0.4784	0.00054	0.00048
0.0953	0.4992	0.00055	0.00049
0.1049	0.5173	0.00056	0.0005
0.1128	0.5345	0.00058	0.00051
0.1212	0.5559	0.00059	0.00052
0.1319	0.5753	0.00061	0.00053
0.1407	0.5904	0.00062	0.00054
0.1505	0.6055	0.00063	0.00055
0.1592	0.6229	0.00065	0.00056

Table 5: G8, 40 deg, 150k Re

C_D	C_L	dC_D	dC_L
0.1359	-0.3456	0.00142	0.00166
0.116	-0.321	0.0014	0.00161
0.099	-0.2948	0.00138	0.00157
0.0762	-0.26	0.00137	0.00152
0.0619	-0.238	0.00136	0.00149
0.0492	-0.2019	0.00135	0.00145
0.0447	-0.1835	0.00135	0.00143
0.0343	-0.1465	0.00134	0.00139
0.0285	-0.1206	0.00134	0.00137
0.0264	-0.0821	0.00133	0.00135
0.0208	-0.0523	0.00133	0.00134
0.0254	-0.0213	0.00133	0.00133
0.0209	0.0067	0.00133	0.00133
0.0239	0.0406	0.00133	0.00133
0.0228	0.0723	0.00133	0.00135
0.0149	0.0952	0.00133	0.00136
0.0217	0.1314	0.00134	0.00138
0.0272	0.1692	0.00134	0.00141
0.0278	0.2013	0.00134	0.00145
0.0342	0.2354	0.00135	0.00149
0.035	0.2626	0.00135	0.00152
0.04	0.3019	0.00136	0.00158
0.0454	0.3303	0.00137	0.00163
0.0481	0.3677	0.00137	0.00169
0.0566	0.3956	0.00138	0.00174
0.0671	0.4215	0.00139	0.00179
0.0753	0.453	0.0014	0.00185
0.0805	0.4733	0.00141	0.00189
0.096	0.494	0.00142	0.00193
0.0976	0.5088	0.00143	0.00196
0.1084	0.5319	0.00144	0.00201
0.1198	0.5565	0.00146	0.00206
0.1272	0.5646	0.00146	0.00208
0.134	0.582	0.00147	0.00212
0.1454	0.6022	0.00149	0.00217
0.1549	0.6173	0.0015	0.0022

Table 6: G8, 40 deg, 300k Re

C_D	C_L	dC_D	dC_L
0.1338	-0.348	0.00046	0.00043
0.1166	-0.3205	0.00044	0.00042
0.0964	-0.2927	0.00042	0.0004
0.0699	-0.2597	0.00041	0.00038
0.0546	-0.2322	0.00039	0.00037
0.0447	-0.1973	0.00038	0.00036
0.038	-0.1672	0.00036	0.00035
0.0322	-0.1379	0.00035	0.00035
0.0277	-0.1047	0.00035	0.00034
0.0241	-0.0689	0.00034	0.00034
0.0213	-0.0318	0.00033	0.00033
0.0194	-0.0049	0.00033	0.00033
0.0176	0.0319	0.00033	0.00033
0.0175	0.0683	0.00034	0.00034
0.0173	0.1005	0.00034	0.00034
0.016	0.1304	0.00035	0.00035
0.0188	0.1618	0.00036	0.00035
0.0223	0.2002	0.00038	0.00036
0.0242	0.2277	0.00039	0.00037
0.0285	0.256	0.0004	0.00038
0.0336	0.2872	0.00042	0.00039
0.0383	0.3146	0.00043	0.0004
0.0423	0.3433	0.00045	0.00041
0.0491	0.3691	0.00046	0.00043
0.0575	0.4063	0.00049	0.00044
0.0668	0.4358	0.00051	0.00046
0.074	0.4599	0.00052	0.00047
0.0801	0.479	0.00054	0.00048
0.089	0.4981	0.00055	0.00049
0.0986	0.5204	0.00057	0.0005
0.1073	0.5428	0.00058	0.00052
0.1176	0.5643	0.0006	0.00053
0.126	0.5785	0.00061	0.00054
0.1342	0.5924	0.00062	0.00055
0.1454	0.6143	0.00064	0.00056
0.1555	0.6308	0.00065	0.00057

Tabe 7: G8, 60 deg, 150k Re

C_D	C_L	dC_D	dC_L
0.1404	-0.3706	0.00143	0.00171
0.1233	-0.348	0.00142	0.00167
0.1027	-0.322	0.0014	0.00163
0.0858	-0.2919	0.00139	0.00158
0.0655	-0.2538	0.00137	0.00152
0.0526	-0.2198	0.00136	0.00148
0.0512	-0.1961	0.00136	0.00145
0.0409	-0.163	0.00135	0.00142
0.0338	-0.1337	0.00135	0.00139
0.0312	-0.0992	0.00134	0.00137
0.0278	-0.0723	0.00134	0.00136
0.0243	-0.0402	0.00134	0.00134
0.021	-0.0021	0.00134	0.00134
0.0208	0.0281	0.00134	0.00134
0.0176	0.0639	0.00134	0.00135
0.0171	0.088	0.00134	0.00136
0.0234	0.1296	0.00135	0.00139
0.0248	0.1648	0.00135	0.00142
0.0301	0.203	0.00135	0.00146
0.0305	0.2381	0.00136	0.0015
0.0369	0.273	0.00136	0.00155
0.0418	0.296	0.00137	0.00158
0.0482	0.3407	0.00138	0.00166
0.055	0.3649	0.00139	0.0017
0.0586	0.401	0.00139	0.00176
0.0642	0.4307	0.0014	0.00182
0.076	0.4596	0.00141	0.00187
0.0844	0.4761	0.00142	0.00191
0.0902	0.4949	0.00143	0.00195
0.1014	0.5153	0.00144	0.00199
0.1118	0.5262	0.00145	0.00201
0.1235	0.5413	0.00146	0.00205
0.1207	0.5579	0.00147	0.00208
0.1351	0.5745	0.00148	0.00212
0.1519	0.6043	0.0015	0.00219
0.1626	0.6182	0.00152	0.00222

Table 8: G8, 60 deg, 300k Re

C_D	C_L	dC_D	dC_L
0.1376	-0.3612	0.00047	0.00044
0.1213	-0.3352	0.00045	0.00042
0.0998	-0.3086	0.00044	0.00041
0.0763	-0.28	0.00042	0.0004
0.0586	-0.2462	0.0004	0.00038
0.0482	-0.218	0.00039	0.00037
0.0414	-0.1843	0.00037	0.00036
0.0349	-0.1502	0.00036	0.00035
0.0298	-0.1171	0.00035	0.00035
0.0257	-0.0809	0.00034	0.00034
0.0216	-0.0415	0.00034	0.00034
0.0197	-0.0033	0.00033	0.00034
0.0182	0.0314	0.00034	0.00034
0.018	0.0681	0.00034	0.00034
0.0164	0.1035	0.00035	0.00034
0.018	0.1402	0.00036	0.00035
0.0203	0.1743	0.00037	0.00036
0.0226	0.2051	0.00038	0.00037
0.0261	0.2393	0.00039	0.00038
0.0292	0.2664	0.00041	0.00039
0.0345	0.2972	0.00042	0.0004
0.0403	0.3305	0.00044	0.00041
0.0458	0.3603	0.00046	0.00042
0.0529	0.3884	0.00048	0.00044
0.0601	0.4197	0.0005	0.00045
0.068	0.4468	0.00052	0.00047
0.0788	0.4788	0.00054	0.00048
0.0853	0.4928	0.00055	0.00049
0.0931	0.5119	0.00056	0.0005
0.1027	0.5316	0.00058	0.00051
0.1121	0.5491	0.00059	0.00052
0.1209	0.5696	0.00061	0.00054
0.1285	0.5836	0.00062	0.00055
0.1393	0.5988	0.00063	0.00056
0.1502	0.62	0.00065	0.00057
0.1613	0.6379	0.00066	0.00058

Table 9: G8, small, 150k Re

C_D	C_L	dC_D	dC_L
0.1207	-0.3088	0.00149	0.0017
0.1085	-0.2965	0.00148	0.00168
0.0894	-0.2609	0.00146	0.00163
0.0772	-0.24	0.00145	0.0016
0.0532	-0.2125	0.00144	0.00156
0.0436	-0.1792	0.00144	0.00152
0.0389	-0.1596	0.00143	0.0015
0.0349	-0.138	0.00143	0.00148
0.0252	-0.1152	0.00143	0.00146
0.0237	-0.091	0.00142	0.00145
0.0219	-0.0666	0.00142	0.00143
0.0206	-0.0474	0.00142	0.00143
0.0162	-0.0245	0.00142	0.00142
0.0172	0.0053	0.00142	0.00142
0.0153	0.0379	0.00142	0.00143
0.0145	0.0685	0.00142	0.00144
0.0203	0.0942	0.00142	0.00145
0.0218	0.1131	0.00143	0.00146
0.0242	0.1352	0.00143	0.00148
0.0236	0.1691	0.00143	0.00151
0.0285	0.206	0.00143	0.00155
0.0301	0.2273	0.00144	0.00158
0.0346	0.2551	0.00144	0.00162
0.0399	0.2733	0.00145	0.00164
0.0434	0.2935	0.00145	0.00168
0.0509	0.331	0.00146	0.00174
0.056	0.3613	0.00146	0.00179
0.063	0.3789	0.00147	0.00183
0.0648	0.3959	0.00147	0.00186
0.0782	0.4229	0.00149	0.00191
0.0851	0.4426	0.00149	0.00195
0.089	0.4669	0.0015	0.002
0.1035	0.4925	0.00152	0.00206
0.1113	0.5082	0.00153	0.00209
0.1165	0.5382	0.00154	0.00216
0.1313	0.5483	0.00155	0.00219

Table 10: G8, small, 300k Re

C_D	C_L	dC_D	dC_L
0.1173	-0.3018	0.00045	0.00043
0.1008	-0.2754	0.00043	0.00042
0.0828	-0.2501	0.00042	0.00041
0.0561	-0.221	0.00041	0.00039
0.0455	-0.2004	0.0004	0.00039
0.0373	-0.165	0.00038	0.00038
0.0315	-0.1402	0.00038	0.00037
0.0265	-0.115	0.00037	0.00037
0.0236	-0.0899	0.00036	0.00036
0.0211	-0.0635	0.00036	0.00036
0.0183	-0.0371	0.00036	0.00036
0.0162	-0.0126	0.00035	0.00035
0.0158	0.02	0.00036	0.00035
0.015	0.0392	0.00036	0.00036
0.0142	0.0676	0.00036	0.00036
0.0147	0.0971	0.00036	0.00036
0.0169	0.1205	0.00037	0.00037
0.0195	0.1453	0.00038	0.00037
0.0216	0.1708	0.00038	0.00038
0.0223	0.1936	0.00039	0.00038
0.0253	0.2164	0.0004	0.00039
0.0301	0.2448	0.00041	0.0004
0.0328	0.2666	0.00042	0.00041
0.0375	0.2885	0.00044	0.00042
0.0428	0.3173	0.00045	0.00043
0.0484	0.3403	0.00046	0.00044
0.0538	0.3674	0.00048	0.00045
0.061	0.3829	0.00049	0.00046
0.0678	0.4102	0.00051	0.00047
0.0757	0.4311	0.00052	0.00049
0.0833	0.4502	0.00053	0.0005
0.0908	0.4681	0.00055	0.00051
0.0994	0.4883	0.00056	0.00052
0.1083	0.5054	0.00057	0.00053
0.1158	0.528	0.00059	0.00054
0.1257	0.5429	0.0006	0.00055

Table 11: G8, med, 150k Re

C_D	C_L	dC_D	dC_L
0.119	-0.2935	0.00144	0.00162
0.1105	-0.29	0.00143	0.00161
0.0965	-0.2702	0.00142	0.00158
0.0744	-0.2394	0.0014	0.00154
0.0606	-0.2147	0.00139	0.00151
0.0472	-0.1843	0.00139	0.00147
0.04	-0.1545	0.00138	0.00144
0.0322	-0.1308	0.00138	0.00142
0.0302	-0.1129	0.00138	0.00141
0.0269	-0.079	0.00137	0.00139
0.0266	-0.0641	0.00137	0.00138
0.0224	-0.0505	0.00137	0.00138
0.0225	-0.024	0.00137	0.00137
0.0182	-0.0017	0.00137	0.00137
0.02	0.0258	0.00137	0.00137
0.0171	0.0499	0.00137	0.00138
0.0128	0.083	0.00137	0.00139
0.0205	0.1031	0.00138	0.0014
0.0227	0.1296	0.00138	0.00142
0.0245	0.1565	0.00138	0.00145
0.0253	0.1831	0.00138	0.00147
0.0292	0.2032	0.00138	0.00149
0.0347	0.2473	0.00139	0.00155
0.0409	0.2635	0.0014	0.00157
0.0434	0.3086	0.0014	0.00164
0.0488	0.3271	0.00141	0.00167
0.0532	0.3386	0.00141	0.00169
0.0586	0.3562	0.00142	0.00172
0.0677	0.3841	0.00142	0.00177
0.0747	0.4172	0.00143	0.00183
0.0746	0.4351	0.00144	0.00187
0.0834	0.4622	0.00145	0.00192
0.1011	0.49	0.00147	0.00198
0.1066	0.5063	0.00147	0.00202
0.1157	0.5328	0.00149	0.00208
0.1212	0.5372	0.00149	0.00209

Table 12: G8, med, 300k Re

C_D	C_L	dC_D	dC_L
0.1088	-0.2891	0.00043	0.00041
0.101	-0.2699	0.00042	0.0004
0.0815	-0.242	0.00041	0.00039
0.056	-0.2147	0.00039	0.00038
0.0447	-0.1908	0.00038	0.00037
0.0371	-0.1617	0.00037	0.00036
0.0333	-0.1439	0.00037	0.00036
0.0278	-0.1184	0.00036	0.00035
0.0243	-0.0932	0.00035	0.00035
0.0221	-0.0672	0.00035	0.00035
0.0198	-0.0355	0.00034	0.00034
0.0175	-0.0064	0.00034	0.00034
0.0158	0.0134	0.00034	0.00034
0.015	0.0399	0.00034	0.00034
0.0147	0.0637	0.00035	0.00035
0.0142	0.0942	0.00035	0.00035
0.0149	0.1178	0.00036	0.00035
0.0171	0.1461	0.00037	0.00036
0.0181	0.1629	0.00037	0.00036
0.0211	0.1883	0.00038	0.00037
0.0239	0.2127	0.00039	0.00038
0.0275	0.2381	0.0004	0.00038
0.0314	0.2625	0.00041	0.00039
0.0366	0.285	0.00042	0.0004
0.0416	0.3152	0.00044	0.00041
0.0471	0.339	0.00045	0.00042
0.0526	0.3624	0.00047	0.00043
0.0593	0.3865	0.00048	0.00045
0.0665	0.4065	0.0005	0.00046
0.0743	0.4293	0.00051	0.00047
0.0811	0.4507	0.00052	0.00048
0.0898	0.4785	0.00054	0.0005
0.0965	0.4946	0.00056	0.0005
0.1059	0.5104	0.00057	0.00051
0.1145	0.5275	0.00058	0.00052
0.1237	0.546	0.00059	0.00054

Table 13: G8, long, 150k Re

C_D	C_L	dC_D	dC_L
0.1195	-0.2777	0.00143	0.00159
0.0983	-0.2656	0.00142	0.00158
0.0897	-0.2528	0.00141	0.00156
0.0725	-0.2309	0.0014	0.00153
0.0516	-0.2016	0.00139	0.00149
0.0436	-0.1742	0.00138	0.00146
0.0387	-0.1562	0.00138	0.00144
0.0312	-0.1351	0.00138	0.00142
0.0299	-0.1036	0.00137	0.0014
0.0263	-0.084	0.00137	0.00139
0.0251	-0.0604	0.00137	0.00138
0.0237	-0.0324	0.00137	0.00137
0.0217	-0.0126	0.00137	0.00137
0.0209	0.0131	0.00137	0.00137
0.0194	0.0255	0.00137	0.00137
0.0234	0.0631	0.00137	0.00138
0.0237	0.0839	0.00137	0.00139
0.0219	0.1102	0.00137	0.00141
0.0215	0.147	0.00138	0.00143
0.0242	0.1712	0.00138	0.00146
0.0237	0.2094	0.00138	0.0015
0.0316	0.2409	0.00139	0.00154
0.0359	0.2649	0.00139	0.00157
0.0398	0.2928	0.0014	0.00161
0.044	0.3252	0.0014	0.00167
0.0536	0.3473	0.00141	0.0017
0.0583	0.377	0.00142	0.00176
0.0587	0.3962	0.00142	0.00179
0.0681	0.4228	0.00143	0.00184
0.0756	0.4383	0.00144	0.00187
0.0873	0.4559	0.00145	0.00191
0.0998	0.4824	0.00146	0.00196
0.1085	0.4955	0.00147	0.00199
0.1161	0.5186	0.00148	0.00204
0.1219	0.5388	0.00149	0.00209
0.1273	0.5506	0.0015	0.00211

Table 14: G8, long, 300k Re

C_D	C_L	dC_D	dC_L
0.1099	-0.2811	0.00043	0.00041
0.0991	-0.2586	0.00042	0.0004
0.0779	-0.2317	0.0004	0.00039
0.0546	-0.2106	0.00039	0.00038
0.0446	-0.1857	0.00038	0.00037
0.0372	-0.1561	0.00037	0.00036
0.0327	-0.1349	0.00036	0.00036
0.0269	-0.1122	0.00036	0.00035
0.0252	-0.0852	0.00035	0.00035
0.0224	-0.0603	0.00035	0.00035
0.0199	-0.0324	0.00034	0.00034
0.018	-0.0033	0.00034	0.00034
0.0164	0.0237	0.00034	0.00034
0.0164	0.0485	0.00035	0.00035
0.0146	0.074	0.00035	0.00035
0.0168	0.1039	0.00036	0.00035
0.0178	0.1258	0.00036	0.00036
0.0189	0.1476	0.00037	0.00036
0.0205	0.1749	0.00038	0.00037
0.0231	0.2	0.00039	0.00037
0.0255	0.2252	0.0004	0.00038
0.0294	0.252	0.00041	0.00039
0.0337	0.2792	0.00042	0.0004
0.0376	0.3061	0.00044	0.00041
0.0423	0.3283	0.00045	0.00042
0.0485	0.3529	0.00046	0.00043
0.056	0.3801	0.00048	0.00044
0.0611	0.4031	0.00049	0.00046
0.0684	0.424	0.00051	0.00047
0.0757	0.4467	0.00052	0.00048
0.085	0.4684	0.00054	0.00049
0.0927	0.4941	0.00056	0.0005
0.101	0.5139	0.00057	0.00052
0.1094	0.529	0.00058	0.00053
0.1188	0.5456	0.00059	0.00054
0.1275	0.5627	0.00061	0.00055

Table 15: G8, front, 150k Re

C_D	C_L	dC_D	dC_L
0.1202	-0.2947	0.00145	0.00163
0.1138	-0.2836	0.00144	0.00161
0.0992	-0.2646	0.00143	0.00159
0.0745	-0.2492	0.00141	0.00156
0.0639	-0.2242	0.00141	0.00153
0.0476	-0.2039	0.0014	0.0015
0.0449	-0.1808	0.0014	0.00148
0.0445	-0.1566	0.00139	0.00146
0.0327	-0.1425	0.00139	0.00144
0.0322	-0.1129	0.00139	0.00142
0.0287	-0.0919	0.00138	0.00141
0.0298	-0.0701	0.00138	0.0014
0.0264	-0.0441	0.00138	0.00139
0.024	-0.0048	0.00138	0.00138
0.0216	0.0082	0.00138	0.00138
0.0274	0.0283	0.00138	0.00138
0.024	0.0569	0.00138	0.00139
0.0294	0.0844	0.00138	0.0014
0.0211	0.1173	0.00138	0.00142
0.0287	0.1491	0.00139	0.00145
0.0309	0.1703	0.00139	0.00147
0.034	0.2048	0.00139	0.00151
0.0359	0.2404	0.0014	0.00155
0.0404	0.2663	0.0014	0.00159
0.0448	0.3019	0.00141	0.00164
0.0499	0.3363	0.00142	0.0017
0.0499	0.3654	0.00142	0.00175
0.0633	0.3871	0.00143	0.00179
0.0699	0.4052	0.00144	0.00182
0.083	0.448	0.00145	0.00191
0.0853	0.4775	0.00146	0.00197
0.0929	0.505	0.00147	0.00203
0.0977	0.5357	0.00148	0.00209
0.1089	0.5644	0.0015	0.00216
0.1244	0.5866	0.00152	0.00221
0.145	0.62	0.00154	0.00229

Table 16: G8, front, 300k Re

C_D	C_L	dC_D	dC_L
0.1202	-0.2825	0.00043	0.00041
0.1117	-0.277	0.00043	0.00041
0.0971	-0.2577	0.00042	0.0004
0.0808	-0.2385	0.00041	0.00039
0.0538	-0.2119	0.00039	0.00038
0.0428	-0.1866	0.00038	0.00037
0.037	-0.1614	0.00037	0.00037
0.0324	-0.1346	0.00036	0.00036
0.0278	-0.1106	0.00036	0.00035
0.0262	-0.0816	0.00035	0.00035
0.024	-0.0553	0.00035	0.00035
0.0225	-0.0298	0.00035	0.00035
0.02	-0.0014	0.00034	0.00034
0.0193	0.0222	0.00034	0.00034
0.0173	0.0471	0.00035	0.00035
0.0188	0.0723	0.00035	0.00035
0.019	0.1011	0.00036	0.00035
0.0201	0.1263	0.00036	0.00036
0.0203	0.1537	0.00037	0.00036
0.0249	0.1805	0.00038	0.00037
0.0274	0.2072	0.00039	0.00038
0.0296	0.2358	0.0004	0.00039
0.0325	0.26	0.00041	0.00039
0.0377	0.2934	0.00043	0.00041
0.0424	0.3209	0.00044	0.00042
0.0479	0.3475	0.00046	0.00043
0.0525	0.3764	0.00048	0.00044
0.06	0.409	0.0005	0.00046
0.0666	0.4367	0.00052	0.00047
0.076	0.4672	0.00054	0.00049
0.0831	0.4908	0.00055	0.0005
0.0917	0.5158	0.00057	0.00052
0.0998	0.5395	0.00059	0.00053
0.1107	0.5673	0.00061	0.00055
0.1224	0.5916	0.00063	0.00056
0.1348	0.6211	0.00065	0.00058

Table 17: G8, mid, 150k Re

C_D	C_L	dC_D	dC_L
0.1202	-0.2825	0.00043	0.00041
0.1117	-0.277	0.00043	0.00041
0.0971	-0.2577	0.00042	0.0004
0.0808	-0.2385	0.00041	0.00039
0.0538	-0.2119	0.00039	0.00038
0.0428	-0.1866	0.00038	0.00037
0.037	-0.1614	0.00037	0.00037
0.0324	-0.1346	0.00036	0.00036
0.0278	-0.1106	0.00036	0.00035
0.0262	-0.0816	0.00035	0.00035
0.024	-0.0553	0.00035	0.00035
0.0225	-0.0298	0.00035	0.00035
0.02	-0.0014	0.00034	0.00034
0.0193	0.0222	0.00034	0.00034
0.0173	0.0471	0.00035	0.00035
0.0188	0.0723	0.00035	0.00035
0.019	0.1011	0.00036	0.00035
0.0201	0.1263	0.00036	0.00036
0.0203	0.1537	0.00037	0.00036
0.0249	0.1805	0.00038	0.00037
0.0274	0.2072	0.00039	0.00038
0.0296	0.2358	0.0004	0.00039
0.0325	0.26	0.00041	0.00039
0.0377	0.2934	0.00043	0.00041
0.0424	0.3209	0.00044	0.00042
0.0479	0.3475	0.00046	0.00043
0.0525	0.3764	0.00048	0.00044
0.06	0.409	0.0005	0.00046
0.0666	0.4367	0.00052	0.00047
0.076	0.4672	0.00054	0.00049
0.0831	0.4908	0.00055	0.0005
0.0917	0.5158	0.00057	0.00052
0.0998	0.5395	0.00059	0.00053
0.1107	0.5673	0.00061	0.00055
0.1224	0.5916	0.00063	0.00056
0.1348	0.6211	0.00065	0.00058

Table 18: G8, mid, 300k Re

C_D	C_L	dC_D	dC_L
0.1178	-0.2831	0.00042	0.0004
0.1022	-0.2679	0.00041	0.00039
0.085	-0.2458	0.0004	0.00038
0.0622	-0.2242	0.00039	0.00037
0.0498	-0.2074	0.00038	0.00036
0.0413	-0.179	0.00037	0.00035
0.0359	-0.1525	0.00036	0.00035
0.0306	-0.1222	0.00035	0.00034
0.0274	-0.1007	0.00034	0.00034
0.0241	-0.0731	0.00034	0.00033
0.0221	-0.0438	0.00033	0.00033
0.0193	-0.0108	0.00033	0.00033
0.0186	0.0199	0.00033	0.00033
0.0185	0.044	0.00033	0.00033
0.0176	0.0676	0.00034	0.00033
0.0164	0.0998	0.00034	0.00034
0.0164	0.1214	0.00035	0.00034
0.0198	0.1523	0.00036	0.00035
0.021	0.1757	0.00036	0.00035
0.0237	0.1989	0.00037	0.00036
0.0271	0.222	0.00038	0.00037
0.0298	0.2541	0.0004	0.00038
0.0352	0.286	0.00041	0.00039
0.0408	0.3148	0.00043	0.0004
0.0484	0.3476	0.00045	0.00041
0.0539	0.3714	0.00046	0.00042
0.0602	0.402	0.00048	0.00044
0.0663	0.4301	0.0005	0.00045
0.0753	0.4491	0.00051	0.00046
0.0828	0.4743	0.00053	0.00047
0.0924	0.5009	0.00055	0.00049
0.1022	0.5217	0.00057	0.0005
0.1125	0.5402	0.00058	0.00051
0.121	0.5609	0.0006	0.00052
0.1336	0.5845	0.00061	0.00054
0.1442	0.6024	0.00063	0.00055

Table 19: G8, back, 150k Re

C_D	C_L	dC_D	dC_L
0.1274	-0.3222	0.00139	0.0016
0.1134	-0.3032	0.00138	0.00157
0.09	-0.2648	0.00136	0.00151
0.0654	-0.2332	0.00134	0.00147
0.0545	-0.2027	0.00133	0.00143
0.0469	-0.1825	0.00133	0.00141
0.04	-0.1576	0.00133	0.00139
0.0374	-0.1354	0.00132	0.00137
0.0318	-0.1069	0.00132	0.00135
0.0252	-0.0755	0.00132	0.00133
0.0233	-0.0485	0.00132	0.00132
0.0231	-0.0323	0.00132	0.00132
0.0271	-0.0068	0.00132	0.00131
0.0289	0.0194	0.00132	0.00131
0.0185	0.0528	0.00132	0.00132
0.0173	0.0664	0.00132	0.00133
0.0256	0.0927	0.00132	0.00134
0.0286	0.1195	0.00132	0.00136
0.0266	0.1401	0.00132	0.00137
0.0283	0.1698	0.00132	0.0014
0.0366	0.1876	0.00133	0.00141
0.0346	0.2151	0.00133	0.00144
0.0381	0.2494	0.00134	0.00149
0.0426	0.2759	0.00134	0.00152
0.0467	0.3019	0.00135	0.00156
0.0584	0.3301	0.00135	0.00161
0.0601	0.3654	0.00136	0.00166
0.0649	0.3773	0.00137	0.00169
0.0746	0.3993	0.00137	0.00172
0.0766	0.4291	0.00138	0.00178
0.0948	0.4485	0.0014	0.00182
0.0966	0.4633	0.0014	0.00185
0.1008	0.4771	0.00141	0.00187
0.1295	0.4834	0.00143	0.00189
0.1128	0.5068	0.00142	0.00193
0.1222	0.5286	0.00143	0.00198

Table 20: G8, back, 300k Re

C_D	C_L	dC_D	dC_L
0.1243	-0.3172	0.00044	0.00041
0.105	-0.2808	0.00042	0.00039
0.0827	-0.2548	0.0004	0.00038
0.057	-0.2229	0.00038	0.00037
0.0466	-0.1988	0.00037	0.00036
0.0393	-0.1702	0.00036	0.00035
0.0349	-0.1483	0.00035	0.00034
0.0293	-0.1205	0.00034	0.00034
0.0253	-0.0976	0.00034	0.00034
0.0222	-0.0691	0.00033	0.00033
0.0193	-0.0384	0.00033	0.00033
0.0183	-0.0128	0.00033	0.00033
0.0193	0.0253	0.00033	0.00033
0.0187	0.0507	0.00033	0.00033
0.0161	0.069	0.00033	0.00033
0.0168	0.0988	0.00034	0.00033
0.0183	0.1273	0.00035	0.00034
0.0216	0.1543	0.00035	0.00035
0.0229	0.1737	0.00036	0.00035
0.0265	0.2027	0.00037	0.00036
0.0292	0.2227	0.00038	0.00036
0.0334	0.254	0.0004	0.00037
0.038	0.2795	0.00041	0.00038
0.0421	0.2991	0.00042	0.00039
0.0467	0.3248	0.00043	0.0004
0.0519	0.3519	0.00045	0.00041
0.0588	0.3792	0.00047	0.00042
0.0656	0.4014	0.00048	0.00043
0.073	0.4252	0.0005	0.00045
0.0789	0.4474	0.00051	0.00046
0.087	0.467	0.00053	0.00047
0.0936	0.4878	0.00054	0.00048
0.1006	0.5034	0.00055	0.00049
0.1149	0.521	0.00057	0.0005
0.1161	0.5397	0.00058	0.00051
0.1248	0.5566	0.00059	0.00052

Appendix B

The following is a sample calculation for the relevant products. The method is reflective of that which is done within the MATLAB code. All processing was done through looping this method of calculation for all data. This example will be for G8, with no winglet, at a Reynolds number of 150k.

$$F_{N,\text{test}} = -0.9282 \text{ N}, \qquad F_{N,\text{grav}} = 0.2091 \text{ N}$$
$$F_{A,\text{test}} = -1.5771 \text{ N}, \qquad F_{A,\text{grav}} = -1.6352 \text{ N}$$
$$\alpha_{\text{test}} = -16.7162^\circ, \qquad \alpha_{\text{grav}} = -16.7280^\circ$$

Calculating force bias:

$$F_N = F_{N,\text{test}} - F_{N,\text{grav}}, \qquad F_A = F_{A,\text{test}} - F_{A,\text{grav}}.$$
$$F_N = -0.9282 - 0.2091 = -1.1373 \text{ N}, \qquad F_A = -1.5771 - (-1.6352) = 0.0581 \text{ N}.$$

Calculating true, offset angle of attack:

$$\alpha_{\text{true}} = \alpha_{\text{test}} - 1.7^\circ$$
$$\alpha_{\text{true}} = -16.7162^\circ - 1.7^\circ = -18.4162^\circ \qquad \text{in radians,} \quad \alpha_{true} = -18.4162\left(\frac{\pi}{180}\right) = -0.3214 \text{ rad}$$

Calculating lift, drag, and rotating forces:

$$L = F_N \cos\alpha_{true} - F_A \sin\alpha_{true}$$
$$D = F_N \sin\alpha_{true} + F_A \cos\alpha_{true}$$
$$L = (-1.1373)(0.9488) \; - \; (0.0581)(-0.3159) = -1.06 \text{ N}$$
$$D = (-1.1373)(-0.3159) \; + \; (0.0581)(0.9488) = 0.414 \text{ N}$$

Calculating density using ambient data:

$$T = 29.6^\circ\text{C} = 302.75 \text{ K}$$
$$p = 96.60 \text{ kPa} = 96600 \text{ Pa}$$
$$Re = 150.2 \times 10^3, \qquad c = 0.1397 \text{ m}, \qquad R = 287.05 \text{ J}/(\text{kg} \cdot \text{K})$$
$$\rho = \frac{p}{RT} = \frac{96600}{(287.05)(302.75)} = 1.11 \text{ kg/m}^3$$

Calculating dynamic viscosity using Sutherland's law:

$$\mu_{\text{ref}} = 1.716 \times 10^{-5} \text{ kg/(m·s)}, \qquad T_{\text{ref}} = 273.15 \text{ K}, \qquad S_{\text{Suth}} = 110.4 \text{ K}$$
$$\mu = \mu_{\text{ref}} \left(\frac{T}{T_{\text{ref}}}\right)^{3/2} \frac{T_{\text{ref}} + S}{T + S}$$
$$\mu = (1.716 \times 10^{-5}) \left(\frac{302.75}{273.15}\right)^{3/2} \frac{273.15 + 110.4}{302.75 + 110.4} = 1.86 \times 10^{-5} \text{ (kg/m·s)}$$

Calculating velocity and dynamic pressure:

$$Re = \frac{\rho V c}{\mu} \qquad \text{solved for V,} \qquad V = \frac{Re\,\mu}{\rho\, c}$$
$$V = \frac{(150.2 \times 10^3)(1.86 \times 10^{-5})}{(1.11)(0.1397)} = 18.016 \text{ m/s}$$

$$q_\infty = \frac{1}{2}\rho V^2 = \frac{1}{2}(1.11)(18.016)^2 = 179.68 \text{ Pa}$$

All together, calculating lift and drag:

$$c = 0.1397 \text{ m}, \ b = 0.1524 \text{ m}$$

$$S = c \cdot b = (0.1397)(0.1524) = 0.02129 \text{ m}^2$$

$$C_L = \frac{L}{q_\infty S}, \qquad C_D = \frac{D}{q_\infty S}$$

$$\boxed{C_L = \frac{-1.0609}{(179.68)(0.02129)} = -0.2773}$$

$$\boxed{C_D = \frac{0.4144}{(179.68)(0.02129)} = 0.1080}$$

Calculating uncertainty:

$$\delta F_N = \delta F_A = 0.005 \text{ N}$$

$$\delta\alpha = 0.05^\circ = 0.05\left(\frac{\pi}{180}\right) \text{ rad}$$

$$\delta q_\infty = 0.5 \text{ Pa}$$

$$\delta C_L = \sqrt{\left(\frac{\partial C_L}{\partial F_N}\,\delta F_N\right)^2 + \left(\frac{\partial C_L}{\partial F_A}\,\delta F_A\right)^2 + \left(\frac{\partial C_L}{\partial \alpha}\,\delta\alpha\right)^2 + \left(\frac{\partial C_L}{\partial q_\infty}\,\delta q_\infty\right)^2}$$

For lift,

$$\frac{\partial C_L}{\partial F_N} = \frac{\cos\alpha}{q_\infty S} = \frac{\cos(8.7266\times10^4)}{(179.68)(0.02129)} = 0.26141$$

$$\frac{\partial C_L}{\partial F_A} = \frac{-\sin\alpha}{q_\infty S} = \frac{-\sin(8.7266\times10^4)}{(179.68)(0.02129)} = -2.2814\times10^{-4}$$

$$\frac{\partial C_L}{\partial \alpha} = \frac{-F_N\sin\alpha - F_A\cos\alpha}{q_\infty S}$$

$$\frac{\partial C_L}{\partial \alpha} = \frac{-(-1.1373)\sin\left(8.726\times10^{-4}\right) - (0.0581)\cos\left(8.726\times10^{-4}\right)}{(179.68)(0.02129)} = -0.01493$$

$$\frac{\partial C_L}{\partial q_\infty} = -\frac{C_L}{q_\infty} = -\frac{-0.2773}{179.68} = 0.00154$$

$$\delta C_L = \sqrt{((0.26141)(0.005))^2 + \left((-2.2814\times10^{-4})(0.005)\right)^2 + \left((-0.012493)(8.7266\times10^{-4})\right)^2 + ((0.00154)(0.5))^2}$$

$$\boxed{\delta C_L = 0.00152}$$

For drag,

$$\frac{\partial C_D}{\partial F_N} = \frac{\sin\alpha}{q_\infty S} = 2.2814\times10^{-4}$$

$$\frac{\partial C_D}{\partial F_A} = \frac{\cos\alpha}{q_\infty S} = 0.26141$$

$$\frac{\partial C_D}{\partial \alpha} = \frac{F_N\cos\alpha - F_A\sin\alpha}{q_\infty S}$$

$$\frac{\delta C_D}{\delta \alpha} = \frac{(-1.1373)\cos\left(8.72664626 \times 10^{-4}\right) - (0.0581)\sin\left(8.72664626 \times 10^{-4}\right)}{(179.68)(0.02129)} = -0.29731$$

$$\frac{\partial C_D}{\partial q_\infty} = -\frac{C_D}{q_\infty} = -\frac{0.108}{179.68} = -6.0107 \times 10^{-4}$$

$$\delta C_D = \sqrt{\left((2.2814 \times 10^{-4})(0.005)\right)^2 + \left((0.26141)(0.005)\right)^2 + \left((-0.29731)(8.7266 \times 10^{-4})\right)^2 + \left((-6.0107 \times 10^{-4})(0.5)\right)^2}$$

$$\boxed{\delta C_D = 0.00136}$$

Appendix C

```
% THE MEAT AND POTATOES! helper function responsible for processing aerodynamic coefficeints
% as well as propegating uncertainty for any given set of winglet data
function out = process_aero_run(gravData, testData, p_amb, T_amb, Re_target)
% PROCESS_AERO_RUN
% gravData, testData : raw CSV arrays (all 14 colum,ns)
% p_amb : ambient/static pressure [Pa]
% T_amb : ambient temperature [K]
% Re_target : Reynolds number for this run (150e3 or 300e3)
%
% Returns struct 'out':
% alpha_set_deg, alpha_true_deg
% L, D
% CL, CD
% q_inf
% Re

    % column indices
    COL_PITCH = 10;
    COL_AXIAL = 7;
    COL_NORMAL = 8;

    % constants
    c = 0.1397; % chord
    b = 0.1524; % span
    S = c * b; % area
    alpha_offset = -1.7; % deg

    R_air = 287.058; % J/(kg*K)

    % Sutherland's law constants (air)
    mu_ref = 1.716e-5; % kg/(m*s)
    T_ref = 273.15; % K
    S_mu = 110.4; % K

    % extra gravity data (Fn, Fa vs alpha_set)
    alpha_g = gravData(:, COL_PITCH); % deg
    FN_g = gravData(:, COL_NORMAL); % N (normal)
    FA_g = gravData(:, COL_AXIAL); % N (axial)

    % extract test data
    alpha_set = testData(:, COL_PITCH); % deg
    FN_raw = testData(:, COL_NORMAL); % N
    FA_raw = testData(:, COL_AXIAL); % N

    % interpolate gravity forces at test angles and subtract
    FN_grav = interp1(alpha_g, FN_g, alpha_set, 'linear', 'extrap');
    FA_grav = interp1(alpha_g, FA_g, alpha_set, 'linear', 'extrap');

    FN = FN_raw - FN_grav;
    FA = FA_raw - FA_grav;

    % correct angle and convert to radians
    alpha_true_deg = alpha_set + alpha_offset;
    alpha_rad = deg2rad(alpha_true_deg);

    % rotate to lift & drag
    L = FN .* cos(alpha_rad) - FA .* sin(alpha_rad);
```

```
    D = FN .* sin(alpha_rad) + FA .* cos(alpha_rad);

    % density and viscosity (from p_amb, T_amb)
    rho = p_amb / (R_air * T_amb); % kg/m^3

    mu = mu_ref * (T_amb/T_ref)^(3/2) * (T_ref + S_mu)/(T_amb + S_mu);

    % velocity from target Re, then q_inf
    V = Re_target * mu / (rho * c); % m/s
    q_inf = 0.5 * rho * V.^2; % Pa

    % aero coefficients
    CL = L ./ (q_inf * S);
    CD = D ./ (q_inf * S);

    % uncertainty in CL and CD (error prop)

    dFN = 0.005; % N
    dFA = 0.005; % N
    dAlpha = 0.05 * pi/180; % rad
    dq = 0.5; % Pa

    % partials for CL
    dCL_dFN = cos(alpha_rad) ./ (q_inf * S);
    dCL_dFA = -sin(alpha_rad) ./ (q_inf * S);
    dCL_dAlpha = (-FN .* sin(alpha_rad) - FA .* cos(alpha_rad)) ./ (q_inf * S);
    dCL_dq = -CL ./ q_inf;

    dCL = sqrt( (dCL_dFN * dFN ).^2 + ...
               (dCL_dFA * dFA ).^2 + ...
               (dCL_dAlpha * dAlpha).^2 + ...
               (dCL_dq * dq ).^2 );

    % partials for CD
    dCD_dFN = sin(alpha_rad) ./ (q_inf * S);
    dCD_dFA = cos(alpha_rad) ./ (q_inf * S);
    dCD_dAlpha = ( FN .* cos(alpha_rad) - FA .* sin(alpha_rad)) ./ (q_inf * S);
    dCD_dq = -CD ./ q_inf;

    dCD = sqrt( (dCD_dFN * dFN ).^2 + ...
               (dCD_dFA * dFA ).^2 + ...
               (dCD_dAlpha * dAlpha).^2 + ...
               (dCD_dq * dq ).^2 );

    % pack output
    out.alpha_set_deg = alpha_set;
    out.alpha_true_deg = alpha_true_deg;
    out.L = L;
    out.D = D;
    out.CL = CL;
    out.CD = CD;
    out.q_inf = q_inf;
    out.Re = Re_target;
    out.dCL = dCL;
    out.dCD = dCD;

end
```

```
function plot_family_CL_alpha(results, family, ReTag, titleText)
% helper function, generates a plot of the lift coefficient vs angle of
% attack for a selected winglet family at a selected reynolds number

figure; hold on;
labels = strings(1, numel(family));

for k = 1:numel(family)
    cfg = family(k);
    idx = find(strcmp([results.name], cfg));

    alpha = results(idx).(ReTag).alpha_true_deg;
    CL = results(idx).(ReTag).CL;
    dCL = results(idx).(ReTag).dCL;

    % vertical error bars for CL
    errorbar(alpha, CL, dCL, 'LineWidth', 1.2, 'LineStyle','-');
    labels(k) = cfg;
end

grid on;
xlabel('Angle of Attack (deg)');
ylabel('C_L');
title(titleText);
legend(labels, 'Location','best');
end
```

```
function plot_family_CL_CD(results, family, ReTag, titleText)
% helper function, generates a drag polar for a selected winglet family at
% a selected reynolds number

figure; hold on;
labels = strings(1, numel(family));

for k = 1:numel(family)
    cfg = family(k);
    idx = find(strcmp([results.name], cfg));

    CL = results(idx).(ReTag).CL;
    CD = results(idx).(ReTag).CD;
    dCL = results(idx).(ReTag).dCL;
    dCD = results(idx).(ReTag).dCD;

    % main curve
    plot(CD, CL, 'LineWidth', 1.2);
    labels(k) = cfg;

    % vertical error bars
    hV = errorbar(CD, CL, dCL, 'LineStyle','none', 'LineWidth', 1.0);
    set(hV, 'HandleVisibility','off');

    % horizontal error bars
    for n = 1:numel(CD)
        xL = CD(n) - dCD(n);
        xR = CD(n) + dCD(n);
        y = CL(n);
        hH = line([xL xR], [y y], 'LineWidth', 1.0);
        set(hH, 'HandleVisibility','off');
    end
end

grid on;
xlabel('C_D');
ylabel('C_L');
title(titleText);
legend(labels, 'Location','best');

end
```

```
% this code is responsible for the marriage of all calculations and plotting. this code used to
% generate all 12 plots at once, though that is not necessary.
clear; close all; clc;
% list of all winglet configurations in order of G8 rows
configs = ["none","20deg","40deg","60deg", ...
          "small","med","long","front","mid","back"];

% load conditions file
cond = readmatrix('G8_Conditions.txt');

% preallocate struct
results = struct();

for i = 1:numel(configs)

    cfg = configs(i);

    % extract ambient conditions
    T_amb = cond(i,2) + 273.15; % K
    p_amb = cond(i,3) * 1000; % Pa
    Re1 = cond(i,4) * 1000; % lower Re
    Re2 = cond(i,5) * 1000; % higher Re

    % build file names
    gravFile = "Lab4_G8_" + cfg + "_grav.csv";
    f150 = "Lab4_G8_" + cfg + "_150k.csv";
    f300 = "Lab4_G8_" + cfg + "_300k.csv";

    % load data
    gravData = readmatrix(gravFile);
    test150 = readmatrix(f150);
    test300 = readmatrix(f300);

    % process both Re
    out150 = process_aero_run(gravData, test150, p_amb, T_amb, Re1);
    out300 = process_aero_run(gravData, test300, p_amb, T_amb, Re2);

    % store into structure
    results(i).name = cfg;
    results(i).Re150 = out150;
    results(i).Re300 = out300;

end

disp('All configs loaded and processed successfully.');

angleFam = ["none","20deg","40deg","60deg"];

lengthFam = ["none","small","med","long"];

locFam = ["none","front","mid","back"];

plot_family_CL_alpha(results, angleFam, "Re150", "Angle Family Re=150k");
... % run plotter function for both Re values, repeat for 3 familes
plot_family_CL_CD(results, angleFam, "Re150", "Drag Polar Angle Family Re=150k");
... % run plotter function for both Re values, repeat for 3 familes
```

Acknowledgments

I'd like to acknowledge whoever ends up grading this Lab. After talking with some peers about the presumed length, I learned that a large majority ended up with reports that were 50-70 pages long. Of course, a majority of this was from data tables in the required appendices, but that is still utterly ridiculous to grade. I'd like to acknowledge myself for locking in and finishing this on a responsible timeline that allowed me to finish other assignments and study for 2 midterms, comfortably, in the span of 5 days. It wasn't fun. To whoever sees this, have a good night! I didn't.

References

[1] Melvin, "G8_conditions.txt" *AEE 361 Laboratory Data*, Arizona State University, 2025. Available on Canvas.
[2] Melvin, "G8_none_grav.csv" *AEE 361 Laboratory Data*, Arizona State University, 2025. Available on Canvas.
[3] Melvin, "G8_none_150k.csv" *AEE 361 Laboratory Data*, Arizona State University, 2025. Available on Canvas.
[4] Melvin, "G8_none_300k.csv" *AEE 361 Laboratory Data*, Arizona State University, 2025. Available on Canvas.
[5] Melvin, "G8_20deg_grav.csv" *AEE 361 Laboratory Data*, Arizona State University, 2025. Available on Canvas.
[6] Melvin, "G8_20deg_150k.csv" *AEE 361 Laboratory Data*, Arizona State University, 2025. Available on Canvas.
[7] Melvin, "G8_20deg_300k.csv" *AEE 361 Laboratory Data*, Arizona State University, 2025. Available on Canvas.
[8] Melvin, "G8_40deg_grav.csv" *AEE 361 Laboratory Data*, Arizona State University, 2025. Available on Canvas.
[9] Melvin, "G8_40deg_150k.csv" *AEE 361 Laboratory Data*, Arizona State University, 2025. Available on Canvas.
[10] Melvin, "G8_40deg_300k.csv" *AEE 361 Laboratory Data*, Arizona State University, 2025. Available on Canvas.
[11] Melvin, "G8_60deg_grav.csv" *AEE 361 Laboratory Data*, Arizona State University, 2025. Available on Canvas.
[12] Melvin, "G8_60deg_150k.csv" *AEE 361 Laboratory Data*, Arizona State University, 2025. Available on Canvas.
[13] Melvin, "G8_60deg_300k.csv" *AEE 361 Laboratory Data*, Arizona State University, 2025. Available on Canvas.
[14] Melvin, "G8_small_grav.csv" *AEE 361 Laboratory Data*, Arizona State University, 2025. Available on Canvas.
[15] Melvin, "G8_small_150k.csv" *AEE 361 Laboratory Data*, Arizona State University, 2025. Available on Canvas.
[16] Melvin, "G8_small_300k.csv" *AEE 361 Laboratory Data*, Arizona State University, 2025. Available on Canvas.
[17] Melvin, "G8_med_grav.csv" *AEE 361 Laboratory Data*, Arizona State University, 2025. Available on Canvas.
[18] Melvin, "G8_med_150k.csv" *AEE 361 Laboratory Data*, Arizona State University, 2025. Available on Canvas.
[19] Melvin, "G8_med_300k.csv" *AEE 361 Laboratory Data*, Arizona State University, 2025. Available on Canvas.
[20] Melvin, "G8_long_grav.csv" *AEE 361 Laboratory Data*, Arizona State University, 2025. Available on Canvas.
[21] Melvin, "G8_long_150k.csv" *AEE 361 Laboratory Data*, Arizona State University, 2025. Available on Canvas.
[22] Melvin, "G8_long_300k.csv" *AEE 361 Laboratory Data*, Arizona State University, 2025. Available on Canvas.
[23] Melvin, "G8_front_grav.csv" *AEE 361 Laboratory Data*, Arizona State University, 2025.

Available on Canvas.
[24] Melvin, “G8_front_150k.csv” *AEE 361 Laboratory Data*, Arizona State University, 2025. Available on Canvas.
[25] Melvin, “G8_front_300k.csv” *AEE 361 Laboratory Data*, Arizona State University, 2025. Available on Canvas.
[26] Melvin, “G8_mid_grav.csv” *AEE 361 Laboratory Data*, Arizona State University, 2025. Available on Canvas.
[27] Melvin, “G8_mid_150k.csv” *AEE 361 Laboratory Data*, Arizona State University, 2025. Available on Canvas.
[28] Melvin, “G8_mid_300k.csv” *AEE 361 Laboratory Data*, Arizona State University, 2025. Available on Canvas.
[29] Melvin, “G8_back_grav.csv” *AEE 361 Laboratory Data*, Arizona State University, 2025. Available on Canvas.
[30] Melvin, “G8_back_150k.csv” *AEE 361 Laboratory Data*, Arizona State University, 2025. Available on Canvas.
[31] Melvin, “G8_back_300k.csv” *AEE 361 Laboratory Data*, Arizona State University, 2025. Available on Canvas.
[32] Aviation Partners Boeing, “Blended Winglet Performance and Program Pricing,” Aviation Partners Boeing, 2023. Available online: https://www.aviationpartnersboeing.com/products_list_prices.php [Accessed 15 Nov. 2025].
[33] "Supercritical Aerofoils," *SKYbrary Aviation Safety*, 2025. Available at: https://skybrary.aero/articles/supercritical-aerofoils [accessed 15 Nov. 2025].